Influence of finite-time Lyapunov exponents on winter precipitation over Iberian Peninsula

Daniel Garaboa-Paz[1], Nieves Lorenzo[2], and Vicente Pérez-Munũzuri[1]

[1]Group of Nonlinear Physics. Faculty of Physics. University of Santiago de Compostela. 15782 Santiago de Compostela, Spain.

[2]Ephyslab. Faculty of Sciences, Campus de Ourense, University of Vigo, 32004 Ourense, Spain.

Correspondence to: V. Pérez-Muñuzuri
(vicente.perez@cesga.es)

Abstract. Seasonal forecasts have improved during the last decades, mostly due to an increase of understanding of the coupled ocean-atmosphere dynamics, and the development of models able to predict the atmosphere variability. Correlations between different teleconnection patterns and severe weather in different parts of the world are constantly evolving and changing have also evolved during the last years. This paper evaluates the connection between winter precipitation over the Iberian Peninsula and the large-scale tropospheric mixing over the eastern Atlantic ocean. Finite-time Lyapunov exponents (FTLE) have been calculated from 1979 to 2008 to evaluate this mixing. Our study suggests that significant negative correlations exist between summer FTLE anomalies and winter precipitation over Portugal and Spain. To understand the mechanisms behind this correlation, summer anomalies of the FTLE have also been correlated to other circulation and temperature patterns as the sea surface temperature (SST), the sea level pressure (SLP) or the geopotential. The East Atlantic (EA) teleconnection index correlates with the summer FTLE anomalies confirming their role as a seasonal predictor for winter precipitation over the Iberian Peninsula.

1 Introduction

Seasonal forecast in mid-latitudes is still an open research field. However, the importance of this scale is relevant for different sectors such as agriculture (Howden et al., 2007; Meza et al., 2008), health (Thomson et al., 2008), energy (García-Morales and Dubus, 2007), or the financial sector (Meza et al., 2008). Most of Europe is located in the mid-latitude belt, where the changing nature of the atmosphere characteristics makes the seasonal climate forecast a difficult task. Thus, any tool to improve the forecast skill is potentially of great interest.

Two of the most important patterns that influence European climate variability are the North Atlantic Oscillation (NAO) and El Niño Southern Oscillation (ENSO) (Visbeck et al., 2003; Brönnimann, 2007). The indices of these large-scale climatic patterns are used as predictors for seasonal forecast over Europe. However, the relationship between NAO and ENSO and the European variability is nonstationary; that is, the strength of the correlation between these two teleconnections and climate anomalies has changed over time. These patterns, though dominant on a large scale, often fail to provide forecast skill in local regions. Precipitation predictability in Europe using NAO and ENSO as predictors is limited due to nonstationary (Vicente-

Serrano and López-Moreno, 2008; Rodríguez-Fonseca et al., 2016). One way to improve the seasonal forecast would be to identify new predictors. Previous works have shown a possible link between the Iberian precipitation and other variables like summer Sea Surface Temperature (SST) anomalies over the north Atlantic basin (Rodríguez-Fonseca and deCastro, 2002; Lorenzo et al., 2010; Hatzaki et al., 2015), other teleconnection patterns (deCastro et al., 2006; Casanueva et al., 2014) or the Euroasian snow cover in autumn (Brands et al., 2014). The storm track activity has been related to the occurrence of extreme events (Lehmann and Coumou, 2015). Changes in mid-latitude circulation can strongly affect the weather events.

The atmosphere large-scale circulation causes mixing of air masses modifying the global moisture distribution, and therefore the rainfall patterns over the continents. One approach to characterize mixing and transport is by calculating Lagrangian trajectories of passive tracers in the atmosphere. Among the different statistics that can be calculated, finite-time Lyapunov exponents (FTLE) measure the separation of two trajectories over time from initially nearby starting points, i.e. the local mixing rates at a finite time (Shadden et al., 2005). Among others, FTLE have been used to identify the presence of barriers to mixing in the atmosphere between the tropics and extratropics (Pierrehumbert and Yang, 1993), to study the zonal stratospheric jet (Beron-Vera et al., 2008), jet-streams (Tang et al., 2010), hurricanes (Rutherford et al., 2012), transient baroclinic eddies (von Hardenberg and Lunkeit, 2002), the spread of plankton blooms (Huhn et al., 2012), the polar vortex (Koh and Legras, 2002), or the atmospheric rivers (Garaboa-Paz et al., 2015).

Our goal in this study is to characterize the rainfall patterns in the Iberian Peninsula as a function of the large-scale tropospheric mixing over the Atlantic ocean. To that end, we have calculated a climatology of FTLE for the period 1979 – 2008. The obtained time series was then correlated with the precipitation over the Iberian Peninsula. Finally, we discuss the obtained results by considering their relationship to the main modes of circulation variability.

2 Methods

2.1 Data

The atmospheric transport has been studied using wind field data retrieved from the European Center for Medium-Range Weather Forecast reanalysis, ERA-Interim (Dee et al., 2011), with a horizontal spatial resolution of 0.7°, a vertical resolution of 100 hPa and a temporal resolution of 6 hours.

Gridded dataset for daily precipitation (mm) from 1979 to 2008 in Iberian Peninsula was used (IB02). This dataset corresponds to the continental area of both Iberian countries on a high resolution (0.2°) grid. It is the combination of two different datasets; PT02 (Belo-Pereira et al., 2011) and SPAIN02 (Herrera et al., 2012).

Yearly anomalies of the SST, geopotential at 500 hPa, sea level pressure (SLP) and wind speed at 200 hPa and 850 hPa for the same period have been used. The SST anomalies have been derived from *The Extended Reconstructed Sea Surface Temperature* (ERSST) dataset which is a global monthly sea surface temperature dataset derived from the International Comprehensive Ocean-Atmosphere Dataset (ICOADS). It has been derived on a $2° \times 2°$ grid with spatial completeness enhanced using statistical methods. This monthly analysis begins in January 1854 continuing nowadays. The newest version of ERSST, version 4, is based on optimally tuned parameters using the latest datasets and improved analysis methods. The geopotential, SLP and wind speed anomalies have been obtained from the National Center of Environmental Prediction (NCEP) reanalysis with a spatial resolution of $2.5° \times 2.5°$. The climatology used for the anomaly plots is for the $1981-2010$ period.

The teleconnection indices NAO, SCA (Scandinavia pattern), EA (East Atlantic pattern), EA/WR (East Atlantic/ West Russia pattern), POL (The Polar/ Eurasia pattern), SOI (Southern Oscillation Index), PNA (Pacific-North American Pattern) and the atmospheric mode AO (Artic Oscillation) were obtained from the Climate Prediction Center (CPC) at NCEP at monthly time scales. The monthly indices were averaged for the seasons JFM, AMJ, JAS and OND from 1979 to 2008. The most representative atmospheric patterns for the Northern Hemisphere were considered in order to analyze their influence on precipitation for the Iberian Peninsula and with the summer FTLEs.

The Pearson correlation coefficient and the Student's t test were used to identify the statistical significance of the correlations between the anomalies of the FTLE and precipitation.

2.2 Finite-Time Lyapunov Exponents (FTLE)

In a longitude-latitude-pressure coordinate system (ϕ,θ,P), the position of an air particle is calculated as,

$$\begin{aligned} \dot{\phi} &= \frac{u}{R\cos(\theta)} \\ \dot{\theta} &= \frac{v}{R} \\ \dot{P} &= w(\phi,\theta,P,t) \end{aligned} \tag{1}$$

where, u, v and w are the eastward, northward and vertical wind components, respectively, and R is the Earth's mean radius. A fine grid of particles with an initial separation of $0.35°$ is uniformly distributed on the 850 hPa level to avoid the interference of most of the turbulence effects from the boundary layer. The layer covers the domain $(\theta,\phi) \in [0,360] \times [-85,85]$ at time instant t_0. Then, 3D Lagrangian simulations have been performed so that particle trajectories are computed integrating Eq. (2) using a 4-th order Runge-Kutta scheme with a fixed time step of $\Delta t = 1.5$ hours, and multilinear interpolation in time and space.

In order to characterize the atmospheric transport, we introduce the finite-time Lyapunov exponents (FTLE), that measure, at a given location, the maximum stretching rate of an infinitesimal fluid parcel over the interval $[t_0, t_0+\tau]$ starting at $\mathbf{r}(t_0) = \mathbf{r_0}$ and ending at $\mathbf{r}(t_0+\tau)$ (Shadden et al., 2005; Sadlo and Peikert, 2007). The integration time τ must be predefined and it has to be long enough to allow trajectories to explore the coherent structures present in the flow. The FTLE fields λ are computed along the trajectories of Lagrangian tracers in the flow as (Peacock and Dabiri, 2010),

$$\lambda(\mathbf{r}_0,t_0,\tau) = \frac{1}{|\tau|}\log\sqrt{\mu_{max}(\tilde{\mathbf{C}}(\mathbf{r}_0))}, \tag{2}$$

where μ_{max} is the maximum eigenvalue of the pull-back Cauchy-Green deformation tensor $\tilde{\mathbf{C}}$ over a sphere (Haller and Beron-Vera, 2012) which does not take into account the deformation due to vertical movement. Repelling (attracting) coherent structures for $\tau > 0$ ($\tau < 0$) can be thought of as finite-time generalizations of the stable (unstable) manifolds of the system. These structures govern the stretching and folding mechanism that control flow mixing. To capture the main synoptic scales, an integration time $\tau = 5$ days was selected which is about the mean length of the typical synoptic time scale in mid-latitudes.

For larger time scales, observed coherent structures are smeared out, while for smaller τ values those structures are not well shaped, and multiple patterns arise.

Ridges in the FTLE field are used to estimate finite time invariant manifolds in the flow that separate dynamically different regions, and organize air masses transport. A positive time direction (forward FTLE) integration leads to identify lines of maximal divergence of air masses. In contrast, a negative time direction integration, leads to identify areas of maximal convergence (backward FTLE).

A 30-years, $1979-2008$, time series of the FTLE field has been computed by following the same steps explained previously, but varying the initial time t_0 in fixed steps $\Delta t_0 = 6$ hours in order to release a new initial tracer grid. Each FTLE field obtained for each advection from $[t_0, t_0+\tau]$ is an element of the time series $\lambda_i = \lambda(\mathbf{r_0}, t_0 + i\Delta t_0, \tau)$.

FTLE anomalies were calculated from the FTLE median for the area between 30°W and 0°W and between 25°N and 65°N for the period $1979-2008$; i.e. $\mathrm{median}\,[<\lambda>_{\mathbf{r_0}}(t)]$. Seasonal composites (averages) of the anomalies (mean - total mean) of the SST, geopotential height and wind speed were obtained from NCEP for the same period. Then, two time series (positive and negative phases) of these seasonal composites were calculated for years with positive/negative summer FTLE anomalies. Finally, maps shown below correspond to the time-averaged mean of both phases.

3 Results

We have studied the transport of air masses in terms of their FTLE from a climatological point of view. Figure 1(a) shows the FTLE for a given time at 850 hPa over the ocean. These structures reflect the large scale advection of air masses which are stretched and folded as wind transport them. The presence of ridges correspond to repelling manifolds where flow diverges. Time averaged FTLE maps for the $1979-2008$ period are shown in Figs. 1(b,c) for seasons January-March and July-September, respectively. As it was expected, in both cases, three latitudinal bands can be clearly identified in coincidence with the large scale atmospheric circulation belts. For mid-latitudes, FTLE values are approximately two times higher than for the equatorial zone and large-scale mixing is generally higher in winter than in summer.

Westerly winds blowing across the Atlantic bring moist air into Europe. As the FTLE can be considered a measure of the large-scale tropospheric mixing (Garaboa-Paz et al., 2015), their role into winter rainfall in the Iberian Peninsula has been considered. Figure 2 shows the ~~lead-~~lag correlation between winter (JFM) precipitation in Iberian Peninsula and the anomalies of the FTLE ~~from the North Atlantic East Ocean~~ for three different seasons through the period $1979-2008$.

The values obtained for the spring (Fig. 2(a)) and autumn (Fig. 2(c)) are not significant. However, the correlations obtained for summer anomalies FTLE values (Fig. 2(b)) show large negative correlations, spatially consistent and statistically significant between the precipitation of the western half of the peninsula and the FTLE. In other words, for larger negative summer FTLE anomalies (low values of the large-scale tropospheric mixing) in the eastern Atlantic ocean, next winter precipitation over the western Iberian Peninsula will also be larger. This result suggests the possibility of using the FTLE as a tool to forecast the occurrence of significantly rainy winters in the considered area with some months in advance.

The summer FTLE time series ~~of the Eastern North Atlantic (ENA) area~~ that show the largest correlation values with the winter precipitation cover approximately the area between 30°W and 0°W and between 25°N and 65°N. The size of this area was varied within the North Atlantic Ocean without modifying significantly the results shown here.

To gain insight into the observed correlations, positive and negative FTLE anomaly maps have been discussed in terms of the atmospheric circulation and the atmosphere-ocean interactions. Spatial patterns of atmospheric circulation and SST anomalies were calculated for the period 1979 − 2008. Previous studies have shown that SST anomalies in certain areas of the subtropical North Atlantic are statistically related to winter precipitation on the IPNA (Iberian Peninsula North Atlantic) region with a five-month lag (Rodríguez-Fonseca and deCastro, 2002).

Figure 3 shows the ratio between the positive (a) and negative (b) summer FTLE anomalies and the summer FTLE mean, respectively, and the summer SST anomalies calculated for the North Atlantic basin (c,d). Large values of the positive FTLE anomalies (a) correspond to a larger activity of the storm track and its displacement to the south during summer, in agreement with a weakening of the Azores anticyclone and negative SST anomalies for the middle North Atlantic Ocean, Fig. 3(c). On the contrary, low values of the negative FTLE anomalies (b) are associated to highs blocking the pass of cold fronts, thus reducing the large-scale atmospheric mixing. This pattern coincides with large positive SST anomalies observed during summer for the mid North Atlantic Ocean, Fig. 3(d). Both figures for SST anomalies (c,d) have a resemblance with the so-called *summer North Atlantic Horseshoe* (HS) SST pattern although displaced to the northwest. Previous works have found a relationship between summer SST anomalies for different areas of the North Atlantic basin and winter precipitation in Europe (Rodríguez-Fonseca and deCastro, 2002; Cassou et al., 2004). In our case, changes in the large-scale tropospheric mixing during summer, measured in terms of the FTLE anomalies and also observed in the summer SST anomalies, are related to the winter precipitation over Spain and Portugal. This result is in agreement with Lehmann and Coumou (2015) and Dong et al. (2013) that observe a strong connection between changes in the mid-latitude circulation and weather events.

Anomaly maps for the geopotential at 500 hPa, Fig. 4, show that positive summer FTLE anomalies correspond to the next winter positive height anomalies occurring over western coast of Europe (a). On the contrary, summer FTLE negative anomalies correspond to next winter trough, that it is a region with relatively lower heights, occurring over the western coast of Europe and in particular over the western Iberian Peninsula (b). These troughs are associated to cloudy conditions and precipitation. A similar pattern is observed for the SLP anomaly patterns (not shown here).

In addition, winter wind speed anomalies for 200 hPa and 850 hPa are shown in Fig. 5. Weaker winds are observed at latitudes between 40°N and 50°N for the anomalies at 200 hPa associated with positive FTLE anomalies (a). This can be related to a weaker than normal jet stream. As the jet stream defines the storm track, a weaker jet stream means that lows traveling the Atlantic do not reach the Iberian Peninsula with the expected frequency. Moreover, taking into account that winds are larger at latitudes $\approx 30°$N (Fig. 5(a)) and that geopotential anomalies show high pressures over the NE Atlantic and low pressures located at NW Atlantic (Fig. 4(a)) we can hypothesize that the meridional variability of the jet stream increases under these circumstances. Figure 5(c), also for positive summer FTLE anomalies, shows low wind speed values at 850 hPa in the trajectory between Caribbean area and the Iberian Peninsula related to a less transport of moisture and cold fronts with less precipitation. Note that easterlies are displaced towards North. Figures 5(b,d) show the inverse situation for negative summer

FTLE anomalies. In Fig. 5(b) there are no significant anomalies in the storm track. Therefore, the jet stream is in its usual location and the Iberian Peninsula is affected by low pressure systems. Note in Fig. 5(d) that for mid-latitudes and 850 hPa, the connection between the Caribbean area and the Iberian Peninsula is reinforced, meaning that rainfall may be stronger associated with the enhancement of the poleward transport of moisture. As well, weaken easterlies are displaced to lower latitudes reinforcing westerlies between the Caribbean area and the Iberian Peninsula.

Finally, summer anomalies of the FTLE and winter precipitation in the Iberian Peninsula have been correlated to different teleconnection patterns. Table 1 summarizes the main results. Note that summer anomalies of the FTLE and summer and autumn EA index correlate ($+/-$, respectively) with a significance greater than 95%, which also correlates with winter rainfall. EA index is the second mode of inter-annual variability of the tropospheric circulation of the North Atlantic. Previous works have found that in southern Europe the EA pattern is at least as important as the NAO for explaining inter-annual variations of sensible climate variables such as air temperatures, sea-surface temperatures, precipitation or wind (Serrano et al., 1999; Saenz et al., 2001; Comas-Bru and McDermott, 2013; Casanueva et al., 2014). Besides, some recent studies suggest that the EA pattern may play a role in positioning the primary North Atlantic storm track (Seierstad et al., 2007; Woollings et al., 2010). Note as well in Table 1 that the autumn SCA pattern also correlates ($-$) with the summer FTLE anomalies although less significant than EA (90% significant), and this pattern influence the winter precipitation. The Scandinavia pattern (SCA) consists of a primary circulation center over Scandinavia, with weaker centers of opposite sign over western Europe and eastern Russia/ western Mongolia. The Scandinavia pattern has been previously referred to as the Eurasia-1 pattern by Barnston and Livezey (1987) and other studies also have shown its influence on the Iberian Peninsula precipitation (deCastro et al., 2006; Casanueva et al., 2014).

4 Conclusions

In the present study, the connection between winter precipitation over the Iberian Peninsula and the finite-time Lyapunov exponents (FTLE) calculated over the eastern Atlantic ocean has been investigated. A significant negative correlation was observed between the summer FTLE anomalies and winter precipitation over the western Iberian Peninsula. The conclusions suggest the possibility of predicting the occurrence of rainy winters using these exponents several months in advance.

Summer anomalies of the FTLE have also been correlated to other circulation and temperature patterns as SST, SLP or the geopotential. In all cases, negative summer FTLE anomalies correspond to well known patterns of precipitation over western Iberian Peninsula. Low values of tropospheric mixing (negative FTLE anomalies) during summer correspond to positive SST anomalies and highs blocking the passage of fronts over the western Europe. However, wind speed, SLP and geopotential anomalies during next winter show the opposite relationship as lows may reach the Iberian Peninsula, in agreement with the negative correlation observed between summer FTLE and winter precipitation. Our results are in agreement with Cayan (1992) who showed a strong dependence between heat flux, SST anomalies and the SLP modes on large spatial scales. The heat flux anomalies, derived from bulk formulations, exhibit large-scale patterns of variability which are related to patterns of sea level pressure (SLP) variability and also to patterns of SST anomalies. In our case, we showed that FTLE anomalies correspond

Table 1. Seasonal correlations between summer FTLE anomalies, winter rainfall and different teleconnection indices; the North Atlantic Oscillation (NAO), the East Atlantic Pattern (EA), the East Atlantic/Western Russia (EA/WR), the Scandinavian Pattern (SCA), the Pacific/North American teleconnection pattern (PNA), the Southern Oscillation Index (SOI), and the Arctic Oscillation (AO). Only significan values are shown. (*) and (**) stand for significances larger than 95% and 90%, respectively.

Summer FTLE							
Season/index	NAO	EA	EA/WR	SCA	PNA	SOI	AO
JFM						-0,24*	
AMJ	0,34**				0,23*		
JAS		0,46**		-0,26*	0,32**		0,25*
OND		-0,54**		-0,27*	-0,30**		0,29*
Winter Rainfall							
Season/index	NAO	EA	EA/WR	SCA	PNA	SOI	AO
JFM	-0,58**		-0,32**	0,69**		0,37**	-0,52**
AMJ				0,27*			
JAS		-0,38**			-0,25*		
OND		0,46**		0,36**			-0,48**

to patterns of SST and SLP variability. In our opinion, large-scale tropospheric mixing drives summer SST anomalies that lead to changes in the next seasons storm tracks, and consequently changes in the location of action centers, Fig. 4 (low and high pressures centers). Finally, the relationship with some teleconnection patterns of the Northern Hemisphere was shown in Table 1. Once more, summer FTLE anomalies correlate with summer and next autumn EA indices which influence on winter rainfall patterns of the Iberian Peninsula.

Acknowledgements. ERA-Interim data were supported by ECMWF. This work was financially supported by Ministerio de Economía y Competitividad and Xunta de Galicia (CGL2013-45932-R, GPC2015/014), and contributions by the COST Action MP1305 and CRETUS Strategic Partnership (AGRUP2015/02). Computational part of this work was done in the Supercomputing Center of Galicia, CESGA. We acknowledge fruitful discussions with J. Eiras-Barca.

References

Barnston, A.G. and Livezey, R.E. Classification, seasonality and persistence of low-frequency atmospheric circulation patterns. *Monthly Weather Review 115*, 1083–1126, 1987.

Belo-Pereira, M., Dutra, E., and Viterbo , P. Evaluation of global precipitation datasets over the Iberian Peninsula, *J. Geophys. Res. 116*, D20101, 2011.

Beron-Vera, F.J., M.G. Brown, Olascoaga, M.J., I.I. Rypina, H. Kocak, and I.A. Udovydchenkov, Zonal jets as transport barriers in planetary atmospheres, *J. Atmos. Sci. 65*, 3316–3326, 2008.

Brands, S., Herrera, S., and Gutiérrez, J.M. Is Eurasian snow cover in October a reliable statistical predictor for the wintertime climate on the Iberian Peninsula? *International Journal of Climatology 345*, 1615–1627, 2014.

Brönnimann, S. The impact of El Niño/Southern Oscillation on European climate, *Review of Geophysics 45*, RG3003, 2007.

Casanueva, A., Rodríguez-Puebla, C., Frías, M.D., and González-Reviriego, N. Variability of extreme precipitation over Europe and its relationships with teleconnection patterns. *Hydrology and Earth System Sciences 18*, 709–725, 2014.

Cassou, C., Deser, C., Terray, L., Hurrell, J.W., and Drevillon, M. Summer Sea Surface Temperature Conditions in the North Atlantic and Their Impact upon the Atmospheric Circulation in Early Winter. *Journal of Climate 17*, 3349–3363, 2004.

Cayan, D.R. Latent and sensible heat flux anomalies over the northern oceans: Driving the sea surface temperature. *J. of Phys. Ocean. 22*, 859–881, 1992.

Comas-Bru, L. and McDermott, F. Impacts of the EA and SCA patterns on the European twentieth century NAO-winter-climate relationships. *Q. J. R. Meteorol. Soc. 140*, 354–679, 2013.

deCastro, M., Lorenzo, M.N., Taboada, J.J., Sarmiento, M., Alvarez, I., Gómez-Gesteira, M. Influence of teleconnection patterns on precipitation variability and on river flow regimes in the Miño River basin (NW Iberian Peninsula). *Clim. Res. 32*, 63–73, 2006.

Dee, D.P., S. M. Uppala, A.J. Simmons, P. Berrisford, P. Poli, S. Kobayashi, U. Andrae, M. A. Balmaseda, G. Balsamo, P. Bauer, P. Bechtold, A. C. M. Beljaars, L. van de Berg, J. Bidlot, N. Bormann, C. Delsol, R. Dragani, M. Fuentes, A.J. Geer, L. Haimberger, S. B. Healy, H. Hersbach, E. V. Holm, L. Isaksen, P. Kallberg, M. Koehler, M. Matricardi, A. P. McNally, B. M. Monge-Sanz, J.J. Morcrette, B.K. Park, C. Peubey, P. de Rosnay, C. Tavolato, J.N. Thepaut, and F. Vitart. The ERA-Interim reanalysis: configuration and performance of the data assimilation system, *Q. J. Roy. Meteo. Soc. 137*, 553–597, 2011.

Dong, B., Sutton, R., Woolings, T., and Hodges, K. Variability of the North Atlantic summer storm track: mechanisms and impacts on European climate. *Environ. Res. Lett. 8*, 034037, 2013.

Garaboa-Paz, D., Eiras-Barca, J., Huhn, F., and Pérez-Muñuzuri, V. Lagrangian coherent structures along atmospheric rivers. *Chaos 25*, 063105, 2015.

García-Morales, M. and Dubus, L. Forecasting precipitation for hydroelectric power management: how to exploit GCM's seasonal ensemble forecasts, *International Journal of Climatology 27*, 1691–1705, 2007.

Haller, G., and Beron-Vera F.J. Geodesic theory of transport barriers in two-dimensional flows. *Physica D 241*, 1680–1702, 2012.

Hatzaki, M. and Renguang, W. The south-eastern Europe winter precipitation variability in relation to the North Atlantic SST. *Atmospheric Research 152*, 61–68, 2015.

Herrera, S., Gutiérrez, J.M., Ancell, R., Pons, M.R., Fías, M.D., and Fernández, J. Development and analysis of a 50-year high-resolution daily gridded precipitation dataset over Spain (Spain02), *Int. J. Climatol. 32*, 74–85, 2012.

Howden, S.M. Soussana, J.F., Tubiello, F.N., Chhetri, N., Dunlop, M., and Meinke, H. Adapting agriculture to climate change, *Proceedings of the National Academy of Science 104*, 19691–19696, 2007.

Huhn, F. von Kameke, A., Pérez-Muñuzuri, V., Olascoaga, M.J., and Beron-Vera, F.J. The impact of advective transport by the South Indian Ocean Countercurrent on the Madagascar plankton bloom, *Geophys. Res. Lett. 39*, L06602, 2012.

Koh, T.Y., and Legras, B. Hyperbolic lines and the stratospheric polar vortex, *Chaos 12*, 382–394, 2002.

Lehmann, J. and Coumou, D. The influence of mid-latitude storm tracks on hot, cold, dry and wet extremes. *Sci. Rep. 5*, 17491, 2015.

Lorenzo, M.N., Iglesias, I., Taboada, J.J., and Gómez-Gesteira, M. Relationship between monthly rainfall in northwest Iberian Peninsula and North Atlantic sea surface temperature. *International Journal of Climatology 30*, 980–990, 2010.

Meza, F.J., Hansen, J.W., and Osgood, D. Economic Value of Seasonal Climate Forecasts for Agriculture: Review of Ex-Ante Assessments and Recommendations for Future Research, *Journal of Applied Meteorology and Climatology 47*, 1269–1286, 2008.

Peacock, T. and Dabiri, J.O. Introduction to Focus Issue: Lagrangian Coherent Structures, *Chaos 20*, 017501, 2010.

Pierrehumbert, R.T., and H. Yang. Global chaotic mixing on isentropic surfaces, *J. Atmos. Sci. 50*(15), 2462–2480, 1993.

Rodríguez-Fonseca, B. and deCastro, M. On the connection between winter anomalous precipitation in the Iberian Peninsula and North West Africa and the summer subtropical Atlantic sea surface temperature *Geophysical Research Letters 29*, 1863, 2002.

Rodríguez-Fonseca, B., Suárez-Moreno, R., Ayarzagüena, B., López-Parages, J., Gómara, I., Villamayor, J., Mohino, E., Losada, T., and Castaño-Tierno, A. A Review of ENSO Influence on the North Atlantic. A Non-Stationary Signal. *Atmosphere 7*, 87, 2016.

Rutherford, B., G. Dangelmayr, and M.T. Montgomery, Lagrangian coherent structures in tropical cyclone intensification, *Atmos. Chem. Phys. 12*(12), 5483–5507, 2012.

Sadlo, F., and Peikert, R. Efficient visualization of Lagrangian coherent structures by filtered AMR ridge extraction, *IEEE Transactions on Visualization and Computer Graphics 13*, 1456–1463, 2007.

Saenz, J., Rodríguez-Puebla, C., Fernández, J., and Zubillaga, J. Interpretation of interannual winter temperature variations over southwestern Europe. *J. Geophys. Res. 106*, 20641–20651, 2001.

Seierstad, I.A., Stephenson, D.B., and Kvamsto, N.G. How useful are teleconnection patterns for explaining variability in extratropical storminess? *Tellus Ser. A 59*, 170–181, 2007.

Serrano, A., García, J.A., Mateos, V.L., Cancillo, M.L., and Garrido, J. Monthly Modes of Variation of Precipitation over the Iberian Peninsula. *J. Climate 12*, 2894–2919, 1999.

Shadden, S.C., Lekien, F., and Marsden, J. Definition and properties of Lagrangian coherent structures from finite-time Lyapunov exponents in two-dimensional aperiodic flows, *Physica D 212*, 271–304, 2005.

Tang, W., M. Mathur, G. Haller, D.C. Hahn, and F.H. Ruggiero, Lagrangian Coherent Structures near a Subtropical Jet Stream, *J. Atmos. Sci. 67*(7), 2307–2319, 2010.

Thomson, M.C., García-Herrera, R., and Beniston, M. eds. Seasonal Forecasts, Climatic Change and Human Health. New York: Springer. 234 pp, 2008.

Vicente-Serrano, S.M., and López-Moreno, J.I. Nonstationary influence of the North Atlantic Oscillation on European precipitation, *J. Geophys. Res. 113*, D20120, 2008.

Visbeck, M., Chassignet, E., Curry, R., Delworth, T., Dickson, B., and Krahmann, G. The Ocean's Response to North Atlantic Oscillation Variability. In: The North Atlantic Oscillation: Climate Significance and Environmental Impact, Hurrell, J.W., Y. Kushnir, G. Ottersen and M. Visbeck (eds) American Geophysical Union: Washington, DC; 113–146, 2003.

von Hardenberg, J., and A.F. Lunkeit, Transient chaotic mixing during a baroclinic life cycle, *Chaos 10*(1), 1054–1500, 2000.

Woollings, T., Hannachi, A., and Hoskins, B. Variability of the North Atlantic eddy-driven jet stream. *Q. J. R. Meteorol. Soc. 136*, 856–868, 2010.

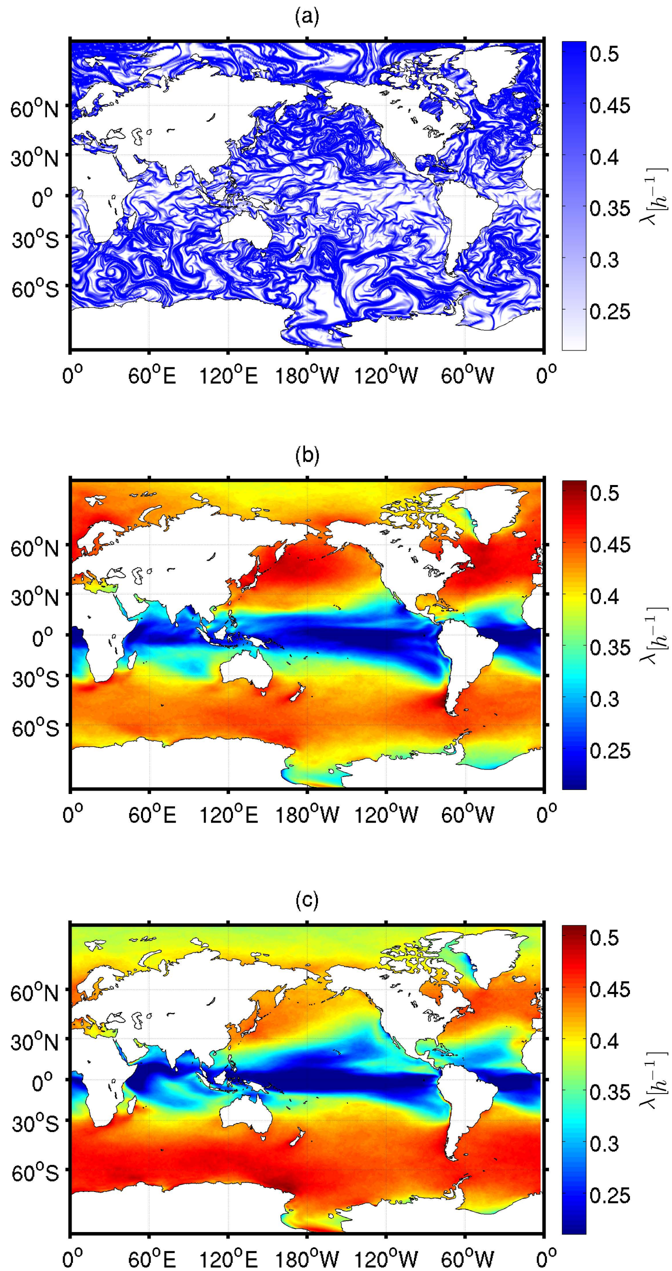

Figure 1. Finite-time Lyapunov exponents λ (a). Local maxima in the plot (darker colors) are potential repelling Lagrangian coherent structures. Mean FTLE climatology for periods January-March (b) and July-September (c) for the $1979 - 2008$ time series. ~~15 days~~.

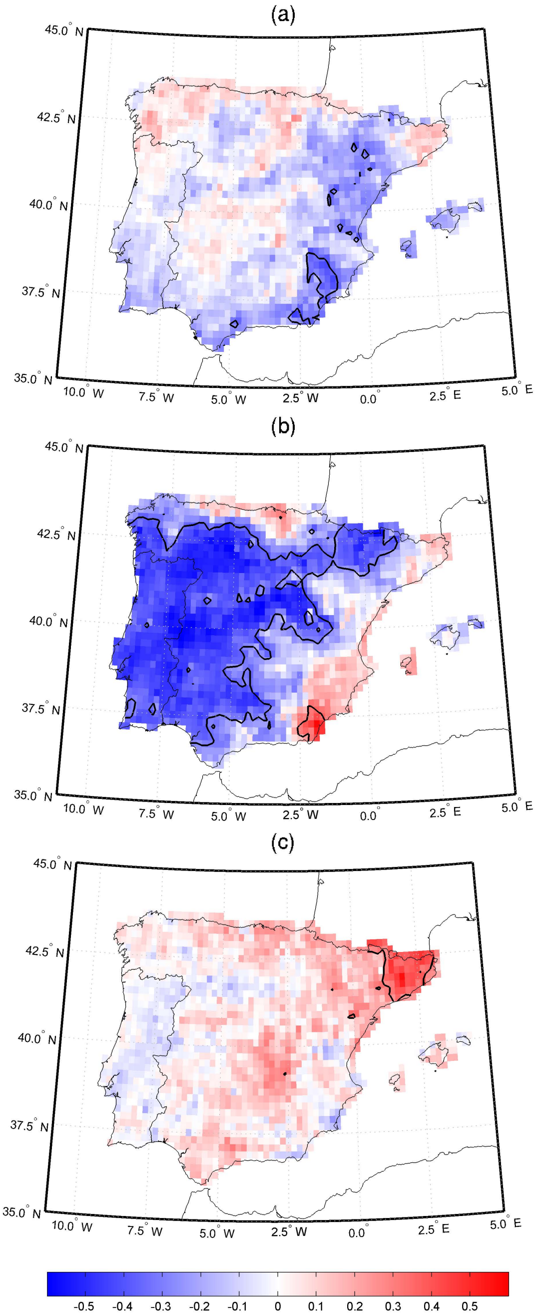

Figure 2. Correlation map between winter precipitation of the Iberian Peninsula and the FTLE anomalies for the Eastern Atlantic region ($[30°W, 0°W] \times [25°N, 65°N]$) for the three previous seasons; a) spring (AMJ), b) summer (JAS) and c) autumn (OND). The black lines mark the significant correlation at 95%.

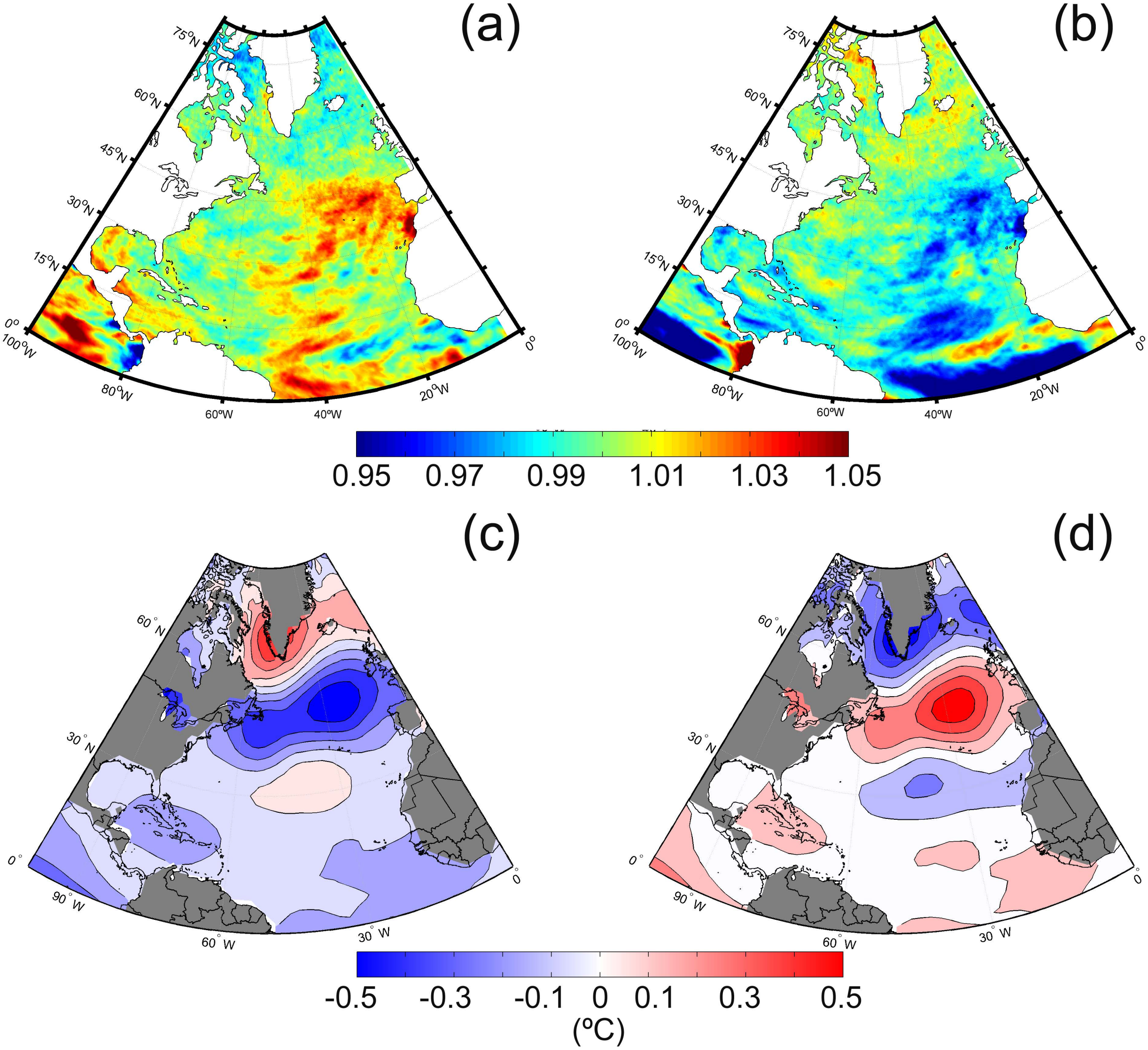

Figure 3. Ratio between the positive (a) and negative (b) summer FTLE anomalies and the global summer FTLE mean. Summer SST anomalies in the Atlantic ocean for years with positive (c) and negative (d) summer FTLE anomalies, respectively.

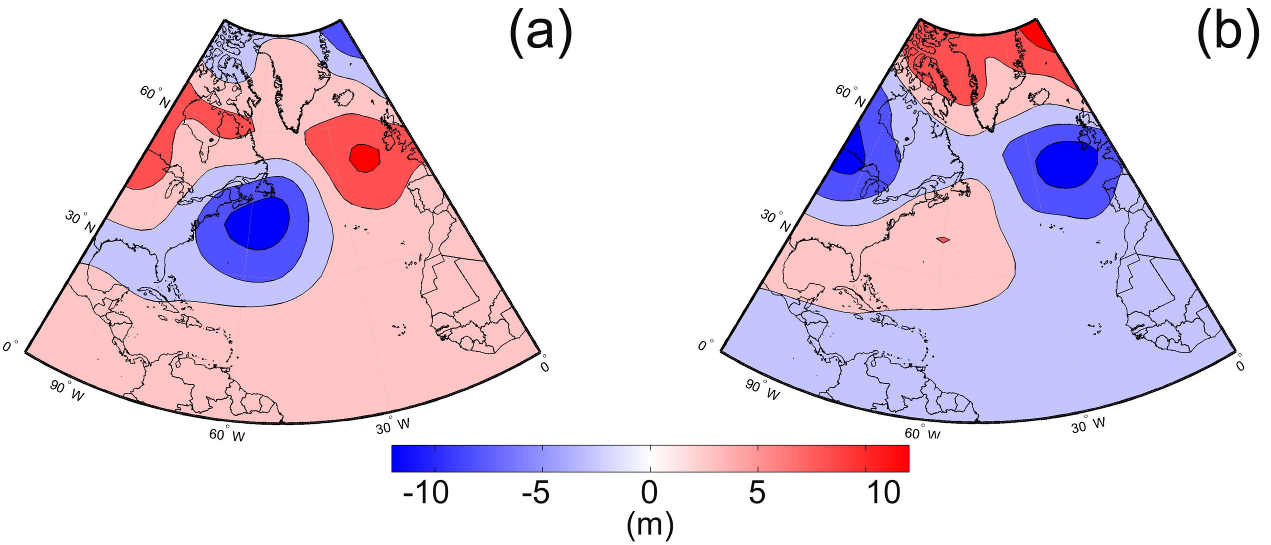

Figure 4. Geopotential at 500 hPa anomalies in the Atlantic for winter. (a) and (b) correspond to years with positive and negative summer FTLE anomalies, respectively.

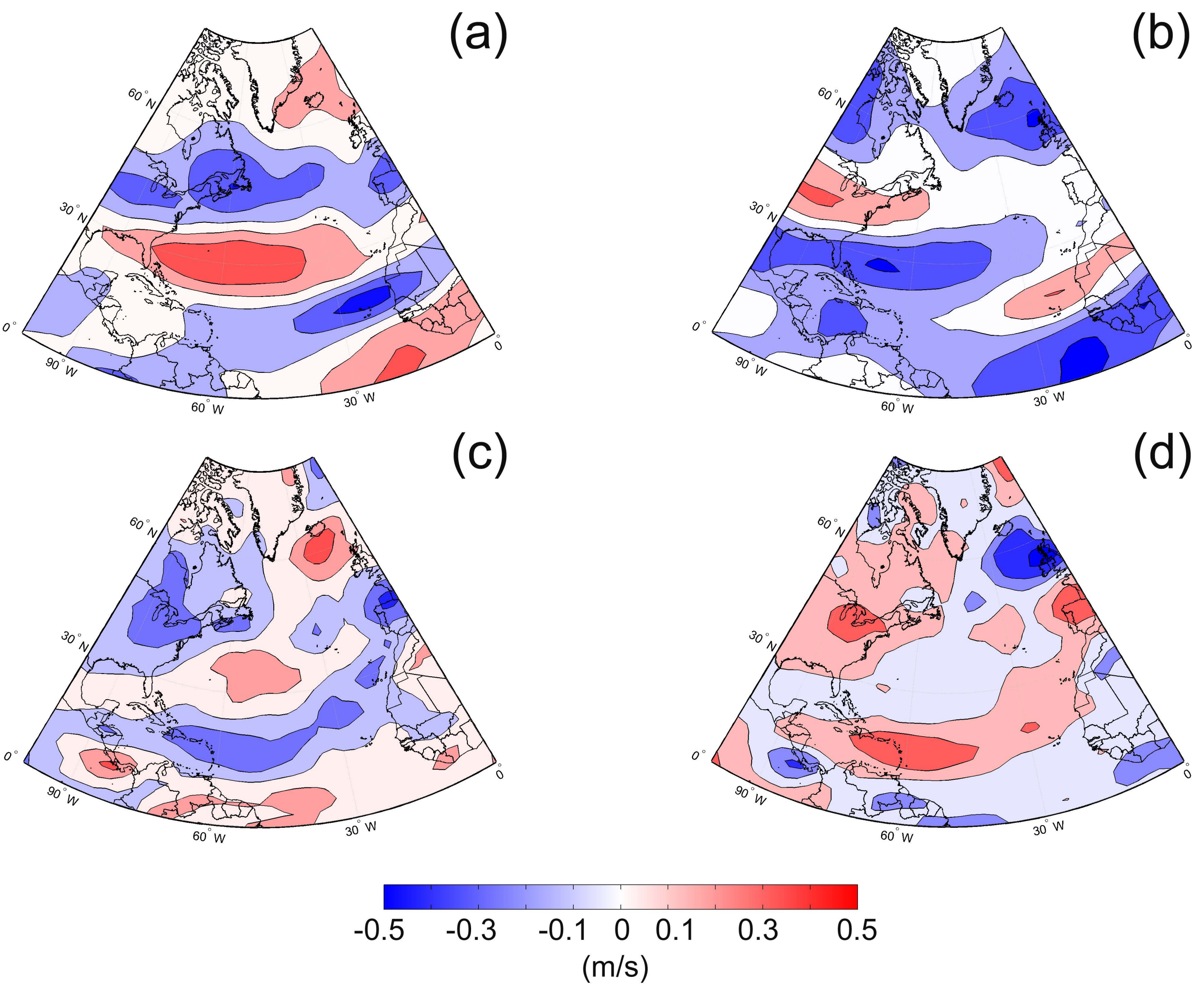

Figure 5. Wind speed anomalies in the Atlantic for winter. (a/b) and (c/d) correspond to years with positive/negative summer FTLE anomalies. Upper and lower maps correspond to 200 hPa and 850 hPa levels, respectively.

We would like to thank the Referee for his/her valuable comments and critics that we tried to take into account in the revised version of the manuscript. Hopefully, all the major and minor corrections pointed out by the reviewer have been corrected now. A detailed answer follows below. We provide replies to the reviewer' comments in bold. As well, corrections included in the manuscript are marked in red.

Answer to Referee 1

The manuscript calculates the local atmospheric mixing using finite time Lyapunov exponents and finds that summertime changes in this field are correlated with winter changes in precipitation over the Iberian Peninsula. Thus, they suggest this field could be used as a predictor of precipitation in this region.

The topic is very relevant and important because seasonal prediction is still a very active area of research. Thus, any advance in this area will be welcome. However, I am not convinced about the interpretation and the mechanism that connects mixing in summer with rainfall in winter. As the authors mention other works have already found a connection between summertime north Atlantic SST and winter rainfall in Europe. Here, the authors try to explain their results expanding on those based on composites.

But, I could not follow the reasoning of the authors: what is the causality link between changes in mixing in summer and rainfall in winter? Through changes in the SST? Does the SST somehow force a certain teleconnection pattern during winter, which in turn changes rainfall?

The interaction between the ocean and atmosphere is complex. Heat and momentum flux at the interface modify currents and winds near the surface. On the other hand, Cayan showed that vast regions of the middle-latitude ocean surface temperature variability is forced by the atmospheric variations. He showed a strong dependence between heat flux, SST anomalies and the SLP modes on spatial scales that often span major portions of the North Atlantic. The heat flux anomalies, derived from bulk formulations, exhibit large-scale patterns of variability which are related to patterns of sea level pressure (SLP) variability and also to patterns of SST anomalies.

In our case, we showed that FTLE anomalies correspond to patterns of SST and SLP variability. In our opinion, large-scale tropospheric mixing drives summer SST anomalies that lead to changes in the next seasons storm tracks, and consequently changes in the location of action centers (low and high pressures centers).

- Cayan, D.R. Latent and sensible heat flux anomalies over the northern oceans: Driving the sea surface temperature. J. of Phys. Ocean. **22**, 859-881, 1992.

Also, changes in mixing are very small, close to 3%... are they significant? Moreover, are the SST, geopotential height, and wind anomalies statistically significant for positive and negative cases of FTLE? Authors need to quantify this, maybe through a test of differences between positive/negative years and neutral years.

Although the changes in the values of positive phase and negative phase of FTLEs are small, the Wilcoxon rank sum test shows that these differences between positive and negative phase of FTLEs are significant. The same is found between the differences of the positive and negative anomalies of the other variables.

Lines 285-287 and 292-295 imply that climatological winds are westerly between the Caribbean and the Iberian Peninsula, but south of 25N the easterly trade winds dominate.

Thus, these sentences are incorrect.

We agree with the reviewer, perhaps in the manuscript we describe Figures 5c and 5d in such a way that they were misunderstood. We have rewritten the corresponding paragraph in the manuscript.

For some particular years, weaken easterlies are displaced to lower latitudes reinforcing westerlies between the Caribbean area and the Iberian Peninsula, meaning that rainfall may be stronger associated with the enhancement of the poleward transport of moisture (see for example, figure for January 2001, a month corresponding to a particularly rainy winter). This situation is a particular case of Fig.5d. However, for other years, easterly winds predominate as they are displaced towards North. Low wind speed values are then observed in the trajectory between Caribbean area and the Iberian Peninsula related to a less frequent arrival of cold fronts and their associated baroclinic structures (see for example, figure for January 2005, a month corresponding to a particularly dry winter). This situation is a particular case of Fig.5c.

January 2001. Particular case for Fig.5d

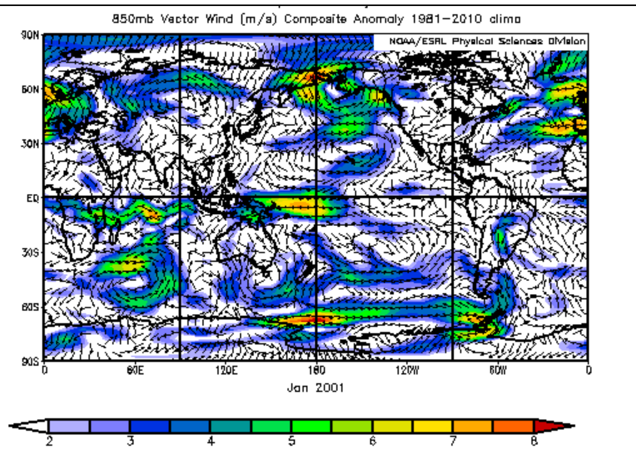

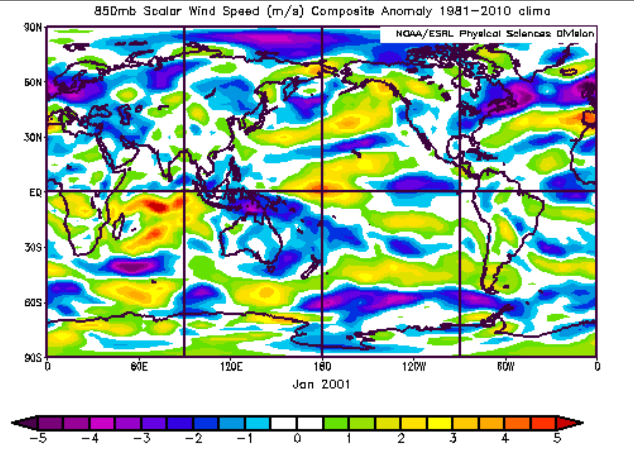

January 2005. Particular case for Fig.5c

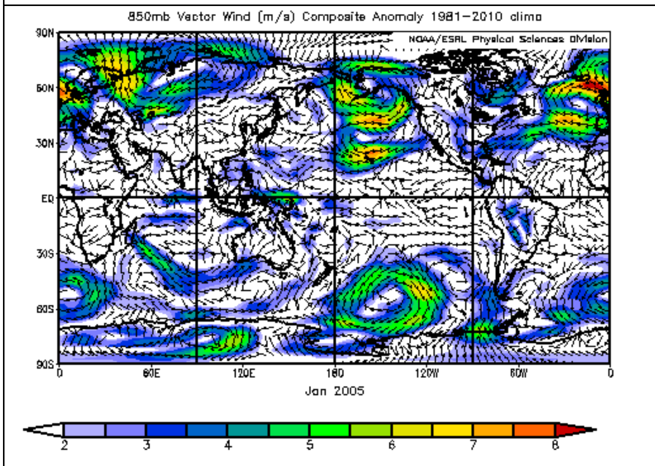

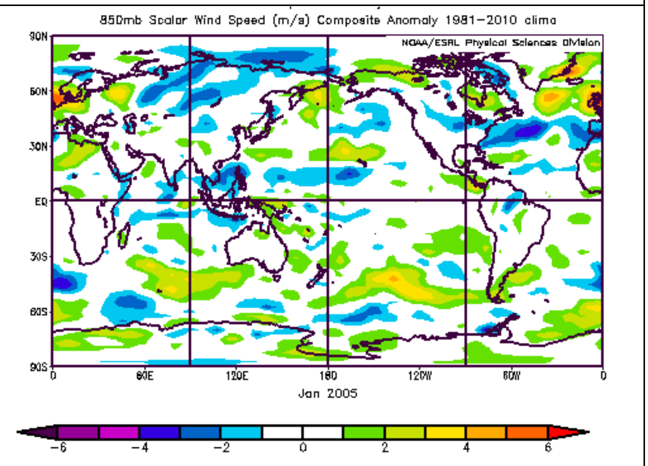

The sentence "less wind than normal" does not sound right. Please change to "weaker winds" or similar.

The reviewer is right. The sentence has been modified.

Why did you choose the 850 hPa level, which is usually just above the boundary layer (PBL)?

We want to focus on the troposphere, but at the same time we wanted to avoid the atmospheric events close to the surface within the PBL. We are interested in the large-scale tropospheric mixing. To that end, we start the advection at the intermediate level of 850hPa so the observed coherent structures are not perturbed by turbulence effects coming from the PBL.

Does mixing change significantly depending on the level?

We perform integrations at different levels 850 hPa, 500 hPa and 300 hPa. In some cases, the main synoptic coherent structures remain qualitatively the same (see for example 3D simulations in Garaboa-Paz et al, 2015) at different levels; the strength of the FTLE ridges diminishes as pressure decreases. We notice that some structures become weaker and the integration time should be modified to capture these structures. However, in some other cases, due to the different flow dynamics occurring at different pressure levels, the observed coherent structures do not coincide. However, we expect the climatological means and anomalies calculated at different levels to behave similarly.

If the deformation due to vertical movement is not taken into consideration, shouldn't you pick a level where the atmosphere tends to behave in 2D? Maybe upper levels?

The particles are advected in 3D, but, only the deformation due to 2D horizontal movement is considered. We want to focus on the horizontal spatial deformation instead of vertical deformation.

The vertical-horizontal scales are completely different in the atmosphere, so considering the deformation due to vertical movement will lead to define a 3x3 Cauchy Green tensor. The eigenvalues of this matrix only take into account the relative deformation of an ellipsoid respect to their initial conditions, without distinction between horizontal or vertical movement. If the vertical deformations have the same weight than horizontal deformation, this could lead to mask the FTLE values.

Why did you chose tau=5 days? Is it to capture the mixing due to synoptic variability? Have you performed a sensitivity test by changing tau within 1 or 2 days?

Yes, the reviewer is right. We want to capture the main synoptic scales. Five days is about the mean length of the typical synoptic time scale in mid-latitudes. For larger time scales, observed coherent structures are smeared out, while for smaller tau values those structures are not well shaped, and multiple patterns arise.

We would like to thank the Referee for his/her valuable comments and critics that we tried to take into account in the revised version of the manuscript. Hopefully, all the major and minor corrections pointed out by the reviewer have been corrected now. A detailed answer follows below. We provide replies to the reviewer' comments in bold. As well, corrections included in the manuscript are marked in red.

Answer to Referee 2

First, the title refers to "seasonal predictability" of winter precipitation, as opposed to "seasonal prediction". This might be a subtle difference, but the readership of Non-linear Processes in Geophysics might wish to distinguish between both aspects. The problem is that I did not really find the "seasonal predictability" (as a nonlinear dynamic characteristic) of the winter precipitation records being quantified (rather, one could argue that the FTLE fields discussed provide a means to quantify the spatio-temporally local predictability of atmospheric flow). I am not convinced that at the considered level of seasonal aggregates, it is even possible to quantify the predictability of seasonal precipitation sums, given the available time span of observations. I also did not find the aspect of "prediction" being specifically addressed at all (which would essentially mean building a regression(?) model for seasonal precipitation sums based on covariates identified by the performed correlation analysis.

We agree with the reviewer, may be the title of the paper is not clear. In this paper, we do not intend to construct a prediction model of winter precipitation based on FTLEs. Our goal is to analyze the potential of FTLEs to see the possibility of considering them as a seasonal prediction tool. So, in order to avoid misunderstandings, we prefer to change the title of the manuscript,

Influence of Finite-time Lyapunov exponents on winter precipitation over Iberian Peninsula

Second, it is appreciated that the authors use dynamical characteristics of the atmospheric circulation to establish a kind of "climatology" in terms of statistical relationships with teleconnection indices. This is most valuable for obtaining a process-based understanding of the observations made. However, it is not clear to me at all why the authors define their four seasons as "JFM", "AMJ", "JAS" and "OND" instead of using the classical - and climatologically well motivated - definitions "DJF", "MAM", "JJA" and "SON". The problem is that when using the terms "summer" and "winter" in the paper, the corresponding definitions do not match what is usually understood by climatologists when using these terms. This makes it hard to establish clear relationships between the findings of the present paper and those of previous works. I strongly recommend revising the results by sticking to the established definitions of seasons.

To our viewpoint there is not a standard definition of seasons. It depends on the scope of the study. Moreover, there exists a large amount of literature where the seasonal periods are defined as we did. Some examples where winter is assimilated to (JFM) are,

- Gastineau G. D’Andrea F. Frankignoul C. (2013) Atmospheric response to the North Atlantic Ocean variability on seasonal to decadal time scales. Clim Dyn (2013) **40**:2311–2330 DOI 10.1007/s00382-012-1333-0
- Picado A, Alvarez I, Vaz N, Varela R, Gómez-Gesteira M, Dias JM. 2014. Assessment of chlorophyll variability along the northwestern coast of Iberian Peninsula. *J. Sea Res.* **93**: 2–11, doi: 10.1016/j.seares.2014.01.008.
- Bamzai A. S. (2003) Relationship between snow cover variability and Arctic oscillation index on a hierarchy of time scales Int. J. Climatol. **23**: 131–142 (2003) doi: 10.1002/joc.854

Third, I recommend giving precise definitions/explanations of how the different types of anomalies used in the paper are calculated. In some cases, this is not obvious from the text and makes evaluating the obtained results quite hard.

We agree with the reviewer, so we add some explanations at the end of the Methods section 2.1. Thanks to point us this.

Seasonal composites (averages) of the anomalies (mean - total mean) of SST, geopotential height and wind speed were obtained from the page (https://www.esrl.noaa.gov/psd/cgi-bin/data/composites) for the period 1979-2008. Total mean make reference to the climatological mean in this case 1981-2010.

Then, two time series (positive and negative phases) of these seasonal composites were calculated for years with positive/negative summer FTLE anomalies. Finally, Figs.(3-5) show the time-averaged mean of both phases.

Fourth, atmospheric circulation is highly dynamic and involves a multiplicity (actually, a continuum) of spatial and temporal scales. I think that it can be justified to restrict the attention within the present work to a single atmospheric layer (850 hPa pressure level) and a constant integration time (5 days; this information should be given in the main text instead of a figure caption), but the motivation of both specific choices should be made transparent. I wonder how much the obtained FTLE fields and established statistical relations may depend on the pressure level at which the tracers are initiated.

We agree with the referee with this insight. We move the information given in the caption to the main text and add some details to clarify this description.

We want to focus on the troposphere, but at the same time we wanted to avoid the atmospheric events close to the surface within the PBL. We are interested in the large-scale tropospheric mixing. To that end, we start the advection at the intermediate level of 850hPa so the observed coherent structures are not perturbed by turbulence effects coming from the PBL.

With respect to the integration time, five days is about the mean length of the typical synoptic time scale in mid-latitudes. For larger time scales, observed coherent structures are smeared out, while for smaller tau values those structures are not well shaped, and multiple patterns arise.

Moreover, how much can we actually learn from time-averaged FTLEs given that Lagrangian coherent structures (LCS), hyperbolic trajectories and related objects embedded in the atmospheric flow are not stationary over the seasonal time scales considered in this work?

Lagrangian coherent structures correspond to flow regions where mixing is larger than the average for a period of tau days. The activity, intensity and presence of these coherent structures in the atmosphere are highly influenced by the atmospheric flow. Their position and shape evolves with time as the flow does. The evolution rate depends on how fast the flow changes as it happens with the rest of atmospheric structures. The FTLE have been widely used in oceanography and meteorology to describe transport phenomena. In our opinion, trying to understand the atmospheric dynamics over the seasonal time scales with the FTLE is equivalent to do it with the SST, SLP, etc. The FTLE describe the amount of large-scale tropospheric mixing available to perturb the SST.

I am willing to accept that the seasonally averaged FTLE fields still provide useful and interpretable information, but what is beyond the mean? For example, does the variance of FTLEs show similar and possibly relevant spatio-temporal patterns? I think that what the authors present is an interesting starting point, but much more could (and should) be done in this regard.

This is an interesting question and we acknowledge the reviewer to point us this idea.

As a first approach, and in a different context, we have performed some simulations to study the variability of the FTLE in terms of the intra-annual (standard deviation of the monthly means for the whole period) and inter-annual (standard deviation of the annual means) variabilities (see pictures below).

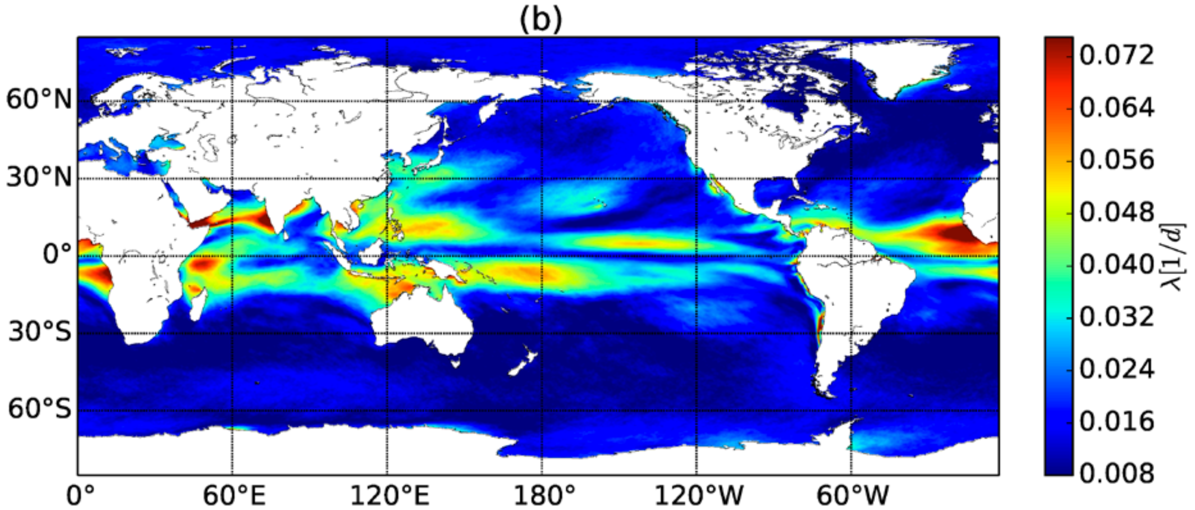

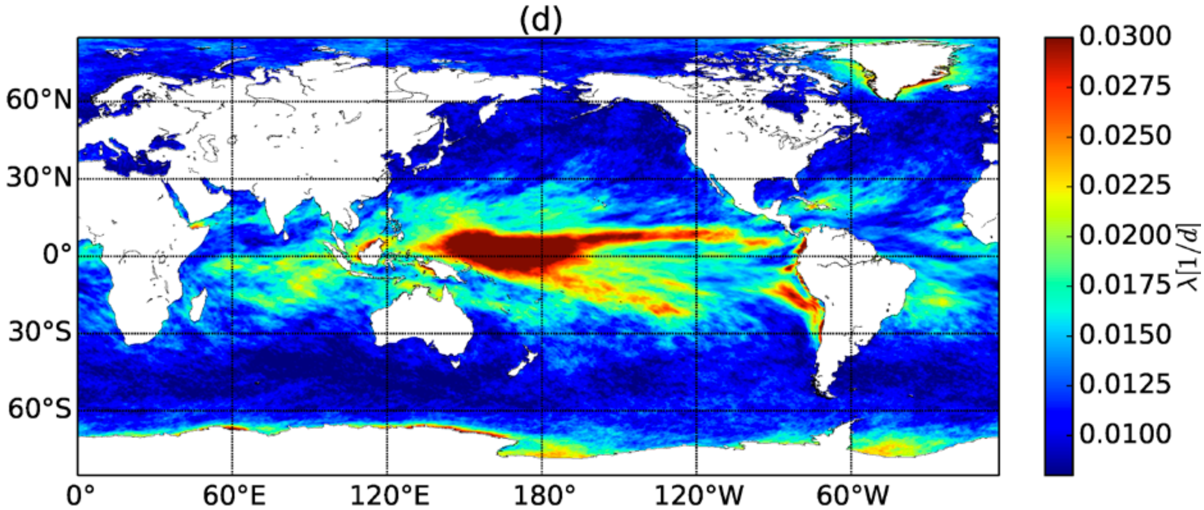

These results highlight El Niño Southern Oscillation, the storm track or the Intertropical Convergence Zone among other large-scale structures.

A time-series consisting of the variance of the FTLEs within the region studied in this manuscript, or the intra or inter-season variabilities of the FTLE could also be used to correlate them with the winter precipitation. However, in our opinion we believe that this study deserves further work and it is beyond the scope of this manuscript.

Finally, the authors just report a relationship between summer mixing and winter precipitation, but I do not find information describing a corresponding physical linkage connecting both seasons. At least some speculations about corresponding mechanisms should be given.

In the Introduction of our manuscript several references were given to previous works that established a possible link between the Iberian precipitation and other variables like summer Sea Surface Temperature (SST) anomalies over the north Atlantic basin (Rodríguez-Fonseca and deCastro, 2002; Lorenzo et al., 2010; Hatzaki et al., 2015), other teleconnection patterns (deCastro et al., 2006; Casanueva et al., 2014) or the Euroasian snow cover in autumn (Brands et al., 2014).

Concerning the mechanisms linking the atmospheric variability with precipitation, we believe that it happens via changes in the SST. The interaction between the ocean and atmosphere is complex. Heat and momentum flux at the interface modify currents and winds near the surface. Cayan showed that vast regions of the middle-latitude ocean surface temperature variability are forced by the atmospheric variations. He showed a strong dependence between heat flux, SST anomalies and the SLP modes on spatial scales that often span major portions of the North Atlantic. The heat flux anomalies, derived from bulk formulations, exhibit large-scale patterns of variability which are related to patterns of sea level pressure (SLP) variability and also to patterns of SST anomalies. In our case, we showed that FTLE anomalies also correspond to patterns of SST and SLP variability. In our opinion, large-scale tropospheric mixing drives summer SST anomalies that lead to changes in the next seasons storm tracks, and consequently changes in the location of action centers (low and high pressures centers).

- Cayan, D.R. Latent and sensible heat flux anomalies over the northern oceans: Driving the sea surface temperature. J. of Phys. Ocean. **22**, 859-881, 1992.

<u>**Specific comments:**</u>

p.1, l.3: Teleconnection patterns and severe weather (events) have not just evolved during the last years, but are constantly changing.

We have modified the Abstract.

When working with wind data, please specific if you consider just the wind speed or the full vector field.

Yes, you are right. We have modified the text. We used the scalar Wind Speed.

p.3, l.10: "the significance of this coefficient was assessed to be greater than 95%" is a quite awkward formulation

We agree with the reviewer. We have modified the text at the end of Section 2.1 as,

The Pearson correlation coefficient and the Student's t test were used to identify the statistical significance of the correlations between the anomalies of the FTLE and precipitation.

p.4, l.19: What do you mean by "lead-lag correlation"?

Lead-lag correlation, describes the situation where one (leading) variable cross-correlated with the values of another (lagging) variable. But, probably you are right and we do not use the correct term, so we changed it to "*lag correlation*".

p.4, l.20: What is the "North Atlantic East Ocean"?

We have modified the manuscript in page 4 at the end of the Methods Section as follow,

FTLE anomalies were calculated from the FTLE median for the area between 30ºW and 0ºW and between 25ºN and 65ºN for the period 1979-2008.

Later on, within the Results section,

Figure 2 shows the lag correlation between winter (JFM) precipitation in Iberian Peninsula and the anomalies of the FTLE for three different seasons through the period 1979-2008.

And,

The summer FTLE time series that show the higher correlation values with the winter precipitation cover approximately the area between 30ºW and 0ºW and between 25ºN and 65ºN. The size of the area chosen to correlate with the precipitation was varied within the North Atlantic Ocean without modifying significantly the results shown here.

p.5, l.1: What is the "IPNA region"?

We agree with the reviewer, IPNA was not defined in the text. IPNA (Iberian Peninsula North Atlantic).

p.5, l.33 and below: Please be specific in whether correlations are positive or negative.

We agree with the reviewer, and the text has been modified including the signs (+) or (-) to account for positive or negative anomalies.

Tab. 1: use capital letters for indicating calendar months

Modified.

p.6, l.9: SCA is not the third leading mode of WINTER SLP variability, but can be computed for all seasons (as every teleconnection index).

You are right, we have modified the text. The Scandinavia pattern (SCAND) consists of a primary circulation center over Scandinavia, with weaker centers of opposite sign over western Europe and eastern Russia/ western Mongolia. The Scandinavia pattern has been previously referred to as the Eurasia-1 pattern by Barnston and Livezey (1987). and other studies also show its influence on the Iberian Peninsula precipitation (deCastro et al., 2006; Casanueva et al., 2014).

In addition, the English could be further polished here and there, especially regarding the proper use of articles and (in just a few cases) the consistency of tenses.

We thank the Referee to point us this problem. We have revised the paper and hopefully the English style has been improved.

Influence of finite-time Lyapunov exponents on winter precipitation over Iberian Peninsula

Daniel Garaboa-Paz[1], Nieves Lorenzo[2], and Vicente Pérez-Munũzuri[1]

[1]Group of Nonlinear Physics. Faculty of Physics. University of Santiago de Compostela. 15782 Santiago de Compostela, Spain.

[2]Ephyslab. Faculty of Sciences, Campus de Ourense, University of Vigo, 32004 Ourense, Spain.

Correspondence to: V. Pérez-Muñuzuri
(vicente.perez@cesga.es)

Abstract. Seasonal forecasts have improved during the last decades, mostly due to an increase of understanding of the coupled ocean-atmosphere dynamics, and the development of models able to predict the atmosphere variability. Correlations between different teleconnection patterns and severe weather in different parts of the world are constantly evolving and changing ~~have also evolved during the last years~~. This paper evaluates the connection between winter precipitation over the Iberian Peninsula and the large-scale tropospheric mixing over the eastern Atlantic ocean. Finite-time Lyapunov exponents (FTLE) have been calculated from 1979 to 2008 to evaluate this mixing. Our study suggests that significant negative correlations exist between summer FTLE anomalies and winter precipitation over Portugal and Spain. To understand the mechanisms behind this correlation, summer anomalies of the FTLE have also been correlated to other circulation and temperature patterns as the sea surface temperature (SST), the sea level pressure (SLP) or the geopotential. The East Atlantic (EA) teleconnection index correlates with the summer FTLE anomalies confirming their role as a seasonal predictor for winter precipitation over the Iberian Peninsula.

1 Introduction

Seasonal forecast in mid-latitudes is still an open research field. However, the importance of this scale is relevant for different sectors such as agriculture (Howden et al., 2007; Meza et al., 2008), health (Thomson et al., 2008), energy (García-Morales and Dubus, 2007), or the financial sector (Meza et al., 2008). Most of Europe is located in the mid-latitude belt, where the changing nature of the atmosphere characteristics makes the seasonal climate forecast a difficult task. Thus, any tool to improve the forecast skill is potentially of great interest.

Two of the most important patterns that influence European climate variability are the North Atlantic Oscillation (NAO) and El Niño Southern Oscillation (ENSO) (Visbeck et al., 2003; Brönnimann, 2007). The indices of these large-scale climatic patterns are used as predictors for seasonal forecast over Europe. However, the relationship between NAO and ENSO and the European variability is nonstationary; that is, the strength of the correlation between these two teleconnections and climate anomalies has changed over time. These patterns, though dominant on a large scale, often fail to provide forecast skill in local regions. Precipitation predictability in Europe using NAO and ENSO as predictors is limited due to nonstationary (Vicente-

Serrano and López-Moreno, 2008; Rodríguez-Fonseca et al., 2016). One way to improve the seasonal forecast would be to identify new predictors. Previous works have shown a possible link between the Iberian precipitation and other variables like summer Sea Surface Temperature (SST) anomalies over the north Atlantic basin (Rodríguez-Fonseca and deCastro, 2002; Lorenzo et al., 2010; Hatzaki et al., 2015), other teleconnection patterns (deCastro et al., 2006; Casanueva et al., 2014) or the Euroasian snow cover in autumn (Brands et al., 2014). The storm track activity has been related to the occurrence of extreme events (Lehmann and Coumou, 2015). Changes in mid-latitude circulation can strongly affect the weather events.

The atmosphere large-scale circulation causes mixing of air masses modifying the global moisture distribution, and therefore the rainfall patterns over the continents. One approach to characterize mixing and transport is by calculating Lagrangian trajectories of passive tracers in the atmosphere. Among the different statistics that can be calculated, finite-time Lyapunov exponents (FTLE) measure the separation of two trajectories over time from initially nearby starting points, i.e. the local mixing rates at a finite time (Shadden et al., 2005). Among others, FTLE have been used to identify the presence of barriers to mixing in the atmosphere between the tropics and extratropics (Pierrehumbert and Yang, 1993), to study the zonal stratospheric jet (Beron-Vera et al., 2008), jet-streams (Tang et al., 2010), hurricanes (Rutherford et al., 2012), transient baroclinic eddies (von Hardenberg and Lunkeit, 2002), the spread of plankton blooms (Huhn et al., 2012), the polar vortex (Koh and Legras, 2002), or the atmospheric rivers (Garaboa-Paz et al., 2015).

Our goal in this study is to characterize the rainfall patterns in the Iberian Peninsula as a function of the large-scale tropospheric mixing over the Atlantic ocean. To that end, we have calculated a climatology of FTLE for the period 1979 – 2008. The obtained time series was then correlated with the precipitation over the Iberian Peninsula. Finally, we discuss the obtained results by considering their relationship to the main modes of circulation variability.

2 Methods

2.1 Data

The atmospheric transport has been studied using wind field data retrieved from the European Center for Medium-Range Weather Forecast reanalysis, ERA-Interim (Dee et al., 2011), with a horizontal spatial resolution of $0.7°$, a vertical resolution of 100 hPa and a temporal resolution of 6 hours.

Gridded dataset for daily precipitation (mm) from 1979 to 2008 in Iberian Peninsula was used (IB02). This dataset corresponds to the continental area of both Iberian countries on a high resolution ($0.2°$) grid. It is the combination of two different datasets; PT02 (Belo-Pereira et al., 2011) and SPAIN02 (Herrera et al., 2012).

Yearly anomalies of the SST, geopotential at 500 hPa, sea level pressure (SLP) and wind speed at 200 hPa and 850 hPa for the same period have been used. The SST anomalies have been derived from *The Extended Reconstructed Sea Surface Temperature* (ERSST) dataset which is a global monthly sea surface temperature dataset derived from the International Comprehensive Ocean-Atmosphere Dataset (ICOADS). It has been derived on a $2° \times 2°$ grid with spatial completeness enhanced using statistical methods. This monthly analysis begins in January 1854 continuing nowadays. The newest version of ERSST, version 4, is based on optimally tuned parameters using the latest datasets and improved analysis methods. The geopotential, SLP and wind speed anomalies have been obtained from the National Center of Environmental Prediction (NCEP) reanalysis with a spatial resolution of $2.5° \times 2.5°$. The climatology used for the anomaly plots is for the $1981-2010$ period.

The teleconnection indices NAO, SCA (Scandinavia pattern), EA (East Atlantic pattern), EA/WR (East Atlantic/ West Russia pattern), POL (The Polar/ Eurasia pattern), SOI (Southern Oscillation Index), PNA (Pacific-North American Pattern) and the atmospheric mode AO (Artic Oscillation) were obtained from the Climate Prediction Center (CPC) at NCEP at monthly time scales. The monthly indices were averaged for the seasons JFM, AMJ, JAS and OND from 1979 to 2008. The most representative atmospheric patterns for the Northern Hemisphere were considered in order to analyze their influence on precipitation for the Iberian Peninsula and with the summer FTLEs.

The Pearson correlation coefficient and the Student's t test were used to identify the statistical significance of the correlations between the anomalies of the FTLE and precipitation.

2.2 Finite-Time Lyapunov Exponents (FTLE)

In a longitude-latitude-pressure coordinate system (ϕ,θ,P), the position of an air particle is calculated as,

$$\begin{aligned}\dot{\phi} &= \frac{u}{R\cos(\theta)} \\ \dot{\theta} &= \frac{v}{R} \\ \dot{P} &= w(\phi,\theta,P,t)\end{aligned} \tag{1}$$

where, u, v and w are the eastward, northward and vertical wind components, respectively, and R is the Earth's mean radius. A fine grid of particles with an initial separation of $0.35°$ is uniformly distributed on the 850 hPa level to avoid the interference of most of the turbulence effects from the boundary layer. The layer covers the domain $(\theta,\phi) \in [0,360]\times[-85,85]$ at time instant t_0. Then, 3D Lagrangian simulations have been performed so that particle trajectories are computed integrating Eq. (2) using a 4-th order Runge-Kutta scheme with a fixed time step of $\Delta t = 1.5$ hours, and multilinear interpolation in time and space.

In order to characterize the atmospheric transport, we introduce the finite-time Lyapunov exponents (FTLE), that measure, at a given location, the maximum stretching rate of an infinitesimal fluid parcel over the interval $[t_0, t_0+\tau]$ starting at $\mathbf{r}(t_0) = \mathbf{r_0}$ and ending at $\mathbf{r}(t_0+\tau)$ (Shadden et al., 2005; Sadlo and Peikert, 2007). The integration time τ must be predefined and it has to be long enough to allow trajectories to explore the coherent structures present in the flow. The FTLE fields λ are computed along the trajectories of Lagrangian tracers in the flow as (Peacock and Dabiri, 2010),

$$\lambda(\mathbf{r}_0,t_0,\tau) = \frac{1}{|\tau|}\log\sqrt{\mu_{max}(\tilde{\mathbf{C}}(\mathbf{r}_0))}, \tag{2}$$

where μ_{max} is the maximum eigenvalue of the pull-back Cauchy-Green deformation tensor $\tilde{\mathbf{C}}$ over a sphere (Haller and Beron-Vera, 2012) which does not take into account the deformation due to vertical movement. Repelling (attracting) coherent structures for $\tau > 0$ ($\tau < 0$) can be thought of as finite-time generalizations of the stable (unstable) manifolds of the system. These structures govern the stretching and folding mechanism that control flow mixing. To capture the main synoptic scales, an integration time $\tau = 5$ days was selected which is about the mean length of the typical synoptic time scale in mid-latitudes.

For larger time scales, observed coherent structures are smeared out, while for smaller τ values those structures are not well shaped, and multiple patterns arise.

Ridges in the FTLE field are used to estimate finite time invariant manifolds in the flow that separate dynamically different regions, and organize air masses transport. A positive time direction (forward FTLE) integration leads to identify lines of maximal divergence of air masses. In contrast, a negative time direction integration, leads to identify areas of maximal convergence (backward FTLE).

A 30-years, $1979-2008$, time series of the FTLE field has been computed by following the same steps explained previously, but varying the initial time t_0 in fixed steps $\Delta t_0 = 6$ hours in order to release a new initial tracer grid. Each FTLE field obtained for each advection from $[t_0, t_0 + \tau]$ is an element of the time series $\lambda_i = \lambda(\mathbf{r_0}, t_0 + i\Delta t_0, \tau)$.

FTLE anomalies were calculated from the FTLE median for the area between 30°W and 0°W and between 25°N and 65°N for the period $1979-2008$; i.e. $\mathrm{median}[<\lambda>_{\mathbf{r_0}}(t)]$. Seasonal composites (averages) of the anomalies (mean - total mean) of the SST, geopotential height and wind speed were obtained from NCEP for the same period. Then, two time series (positive and negative phases) of these seasonal composites were calculated for years with positive/negative summer FTLE anomalies. Finally, maps shown below correspond to the time-averaged mean of both phases.

3 Results

We have studied the transport of air masses in terms of their FTLE from a climatological point of view. Figure 1(a) shows the FTLE for a given time at 850 hPa over the ocean. These structures reflect the large scale advection of air masses which are stretched and folded as wind transport them. The presence of ridges correspond to repelling manifolds where flow diverges. Time averaged FTLE maps for the $1979-2008$ period are shown in Figs. 1(b,c) for seasons January-March and July-September, respectively. As it was expected, in both cases, three latitudinal bands can be clearly identified in coincidence with the large scale atmospheric circulation belts. For mid-latitudes, FTLE values are approximately two times higher than for the equatorial zone and large-scale mixing is generally higher in winter than in summer.

Westerly winds blowing across the Atlantic bring moist air into Europe. As the FTLE can be considered a measure of the large-scale tropospheric mixing (Garaboa-Paz et al., 2015), their role into winter rainfall in the Iberian Peninsula has been considered. Figure 2 shows the ~~lead-~~lag correlation between winter (JFM) precipitation in Iberian Peninsula and the anomalies of the FTLE ~~from the North Atlantic East Ocean~~ for three different seasons through the period $1979-2008$.

The values obtained for the spring (Fig. 2(a)) and autumn (Fig. 2(c)) are not significant. However, the correlations obtained for summer anomalies FTLE values (Fig. 2(b)) show large negative correlations, spatially consistent and statistically significant between the precipitation of the western half of the peninsula and the FTLE. In other words, for larger negative summer FTLE anomalies (low values of the large-scale tropospheric mixing) in the eastern Atlantic ocean, next winter precipitation over the western Iberian Peninsula will also be larger. This result suggests the possibility of using the FTLE as a tool to forecast the occurrence of significantly rainy winters in the considered area with some months in advance.

The summer FTLE time series ~~of the Eastern North Atlantic (ENA) area~~ that show the largest correlation values with the winter precipitation cover approximately the area between 30°W and 0°W and between 25°N and 65°N. The size of this area was varied within the North Atlantic Ocean without modifying significantly the results shown here.

To gain insight into the observed correlations, positive and negative FTLE anomaly maps have been discussed in terms of the atmospheric circulation and the atmosphere-ocean interactions. Spatial patterns of atmospheric circulation and SST anomalies were calculated for the period 1979 – 2008. Previous studies have shown that SST anomalies in certain areas of the subtropical North Atlantic are statistically related to winter precipitation on the IPNA (Iberian Peninsula North Atlantic) region with a five-month lag (Rodríguez-Fonseca and deCastro, 2002).

Figure 3 shows the ratio between the positive (a) and negative (b) summer FTLE anomalies and the summer FTLE mean, respectively, and the summer SST anomalies calculated for the North Atlantic basin (c,d). Large values of the positive FTLE anomalies (a) correspond to a larger activity of the storm track and its displacement to the south during summer, in agreement with a weakening of the Azores anticyclone and negative SST anomalies for the middle North Atlantic Ocean, Fig. 3(c). On the contrary, low values of the negative FTLE anomalies (b) are associated to highs blocking the pass of cold fronts, thus reducing the large-scale atmospheric mixing. This pattern coincides with large positive SST anomalies observed during summer for the mid North Atlantic Ocean, Fig. 3(d). Both figures for SST anomalies (c,d) have a resemblance with the so-called *summer North Atlantic Horseshoe* (HS) SST pattern although displaced to the northwest. Previous works have found a relationship between summer SST anomalies for different areas of the North Atlantic basin and winter precipitation in Europe (Rodríguez-Fonseca and deCastro, 2002; Cassou et al., 2004). In our case, changes in the large-scale tropospheric mixing during summer, measured in terms of the FTLE anomalies and also observed in the summer SST anomalies, are related to the winter precipitation over Spain and Portugal. This result is in agreement with Lehmann and Coumou (2015) and Dong et al. (2013) that observe a strong connection between changes in the mid-latitude circulation and weather events.

Anomaly maps for the geopotential at 500 hPa, Fig. 4, show that positive summer FTLE anomalies correspond to the next winter positive height anomalies occurring over western coast of Europe (a). On the contrary, summer FTLE negative anomalies correspond to next winter trough, that it is a region with relatively lower heights, occurring over the western coast of Europe and in particular over the western Iberian Peninsula (b). These troughs are associated to cloudy conditions and precipitation. A similar pattern is observed for the SLP anomaly patterns (not shown here).

In addition, winter wind speed anomalies for 200 hPa and 850 hPa are shown in Fig. 5. Weaker winds are observed at latitudes between 40°N and 50°N for the anomalies at 200 hPa associated with positive FTLE anomalies (a). This can be related to a weaker than normal jet stream. As the jet stream defines the storm track, a weaker jet stream means that lows traveling the Atlantic do not reach the Iberian Peninsula with the expected frequency. Moreover, taking into account that winds are larger at latitudes $\approx 30°$N (Fig. 5(a)) and that geopotential anomalies show high pressures over the NE Atlantic and low pressures located at NW Atlantic (Fig. 4(a)) we can hypothesize that the meridional variability of the jet stream increases under these circumstances. Figure 5(c), also for positive summer FTLE anomalies, shows low wind speed values at 850 hPa in the trajectory between Caribbean area and the Iberian Peninsula related to a less transport of moisture and cold fronts with less precipitation. Note that easterlies are displaced towards North. Figures 5(b,d) show the inverse situation for negative summer

FTLE anomalies. In Fig. 5(b) there are no significant anomalies in the storm track. Therefore, the jet stream is in its usual location and the Iberian Peninsula is affected by low pressure systems. Note in Fig. 5(d) that for mid-latitudes and 850 hPa, the connection between the Caribbean area and the Iberian Peninsula is reinforced, meaning that rainfall may be stronger associated with the enhancement of the poleward transport of moisture. As well, weaken easterlies are displaced to lower latitudes reinforcing westerlies between the Caribbean area and the Iberian Peninsula.

Finally, summer anomalies of the FTLE and winter precipitation in the Iberian Peninsula have been correlated to different teleconnection patterns. Table 1 summarizes the main results. Note that summer anomalies of the FTLE and summer and autumn EA index correlate (+/−, respectively) with a significance greater than 95%, which also correlates with winter rainfall. EA index is the second mode of inter-annual variability of the tropospheric circulation of the North Atlantic. Previous works have found that in southern Europe the EA pattern is at least as important as the NAO for explaining inter-annual variations of sensible climate variables such as air temperatures, sea-surface temperatures, precipitation or wind (Serrano et al., 1999; Saenz et al., 2001; Comas-Bru and McDermott, 2013; Casanueva et al., 2014). Besides, some recent studies suggest that the EA pattern may play a role in positioning the primary North Atlantic storm track (Seierstad et al., 2007; Woollings et al., 2010). Note as well in Table 1 that the autumn SCA pattern also correlates (−) with the summer FTLE anomalies although less significant than EA (90% significant), and this pattern influence the winter precipitation. The Scandinavia pattern (SCA) consists of a primary circulation center over Scandinavia, with weaker centers of opposite sign over western Europe and eastern Russia/ western Mongolia. The Scandinavia pattern has been previously referred to as the Eurasia-1 pattern by Barnston and Livezey (1987) and other studies also have shown its influence on the Iberian Peninsula precipitation (deCastro et al., 2006; Casanueva et al., 2014).

4 Conclusions

In the present study, the connection between winter precipitation over the Iberian Peninsula and the finite-time Lyapunov exponents (FTLE) calculated over the eastern Atlantic ocean has been investigated. A significant negative correlation was observed between the summer FTLE anomalies and winter precipitation over the western Iberian Peninsula. The conclusions suggest the possibility of predicting the occurrence of rainy winters using these exponents several months in advance.

Summer anomalies of the FTLE have also been correlated to other circulation and temperature patterns as SST, SLP or the geopotential. In all cases, negative summer FTLE anomalies correspond to well known patterns of precipitation over western Iberian Peninsula. Low values of tropospheric mixing (negative FTLE anomalies) during summer correspond to positive SST anomalies and highs blocking the passage of fronts over the western Europe. However, wind speed, SLP and geopotential anomalies during next winter show the opposite relationship as lows may reach the Iberian Peninsula, in agreement with the negative correlation observed between summer FTLE and winter precipitation. Our results are in agreement with Cayan (1992) who showed a strong dependence between heat flux, SST anomalies and the SLP modes on large spatial scales. The heat flux anomalies, derived from bulk formulations, exhibit large-scale patterns of variability which are related to patterns of sea level pressure (SLP) variability and also to patterns of SST anomalies. In our case, we showed that FTLE anomalies correspond

Table 1. Seasonal correlations between summer FTLE anomalies, winter rainfall and different teleconnection indices; the North Atlantic Oscillation (NAO), the East Atlantic Pattern (EA), the East Atlantic/Western Russia (EA/WR), the Scandinavian Pattern (SCA), the Pacific/North American teleconnection pattern (PNA), the Southern Oscillation Index (SOI), and the Arctic Oscillation (AO). Only significan values are shown. (*) and (**) stand for significances larger than 95% and 90%, respectively.

Summer FTLE							
Season/index	NAO	EA	EA/WR	SCA	PNA	SOI	AO
JFM						-0,24*	
AMJ	0,34**				0,23*		
JAS		0,46**		-0,26*	0,32**		0,25*
OND		-0,54**		-0,27*	-0,30**		0,29*
Winter Rainfall							
Season/index	NAO	EA	EA/WR	SCA	PNA	SOI	AO
JFM	-0,58**		-0,32**	0,69**		0,37**	-0,52**
AMJ				0,27*			
JAS		-0,38**			-0,25*		
OND		0,46**		0,36**			-0,48**

to patterns of SST and SLP variability. In our opinion, large-scale tropospheric mixing drives summer SST anomalies that lead to changes in the next seasons storm tracks, and consequently changes in the location of action centers, Fig. 4 (low and high pressures centers). Finally, the relationship with some teleconnection patterns of the Northern Hemisphere was shown in Table 1. Once more, summer FTLE anomalies correlate with summer and next autumn EA indices which influence on winter rainfall patterns of the Iberian Peninsula.

Acknowledgements. ERA-Interim data were supported by ECMWF. This work was financially supported by Ministerio de Economía y Competitividad and Xunta de Galicia (CGL2013-45932-R, GPC2015/014), and contributions by the COST Action MP1305 and CRETUS Strategic Partnership (AGRUP2015/02). Computational part of this work was done in the Supercomputing Center of Galicia, CESGA. We acknowledge fruitful discussions with J. Eiras-Barca.

References

Barnston, A.G. and Livezey, R.E. Classification, seasonality and persistence of low-frequency atmospheric circulation patterns. *Monthly Weather Review 115*, 1083–1126, 1987.

Belo-Pereira, M., Dutra, E., and Viterbo , P. Evaluation of global precipitation datasets over the Iberian Peninsula, *J. Geophys. Res. 116*, D20101, 2011.

Beron-Vera, F.J., M.G. Brown, Olascoaga, M.J., I.I. Rypina, H. Kocak, and I.A. Udovydchenkov, Zonal jets as transport barriers in planetary atmospheres, *J. Atmos. Sci. 65*, 3316–3326, 2008.

Brands, S., Herrera, S., and Gutiérrez, J.M. Is Eurasian snow cover in October a reliable statistical predictor for the wintertime climate on the Iberian Peninsula? *International Journal of Climatology 345*, 1615–1627, 2014.

Brönnimann, S. The impact of El Niño/Southern Oscillation on European climate, *Review of Geophysics 45*, RG3003, 2007.

Casanueva, A., Rodríguez-Puebla, C., Frías, M.D., and González-Reviriego, N. Variability of extreme precipitation over Europe and its relationships with teleconnection patterns. *Hydrology and Earth System Sciences 18*, 709–725, 2014.

Cassou, C., Deser, C., Terray, L., Hurrell, J.W., and Drevillon, M. Summer Sea Surface Temperature Conditions in the North Atlantic and Their Impact upon the Atmospheric Circulation in Early Winter. *Journal of Climate 17*, 3349–3363, 2004.

Cayan, D.R. Latent and sensible heat flux anomalies over the northern oceans: Driving the sea surface temperature. *J. of Phys. Ocean. 22*, 859–881, 1992.

Comas-Bru, L. and McDermott, F. Impacts of the EA and SCA patterns on the European twentieth century NAO-winter-climate relationships. *Q. J. R. Meteorol. Soc. 140*, 354–679, 2013.

deCastro, M., Lorenzo, M.N., Taboada, J.J., Sarmiento, M., Alvarez, I., Gómez-Gesteira, M. Influence of teleconnection patterns on precipitation variability and on river flow regimes in the Miño River basin (NW Iberian Peninsula). *Clim. Res. 32*, 63–73, 2006.

Dee, D.P., S. M. Uppala, A.J. Simmons, P. Berrisford, P. Poli, S. Kobayashi, U. Andrae, M. A. Balmaseda, G. Balsamo, P. Bauer, P. Bechtold, A. C. M. Beljaars, L. van de Berg, J. Bidlot, N. Bormann, C. Delsol, R. Dragani, M. Fuentes, A.J. Geer, L. Haimberger, S. B. Healy, H. Hersbach, E. V. Holm, L. Isaksen, P. Kallberg, M. Koehler, M. Matricardi, A. P. McNally, B. M. Monge-Sanz, J.J. Morcrette, B.K. Park, C. Peubey, P. de Rosnay, C. Tavolato, J.N. Thepaut, and F. Vitart. The ERA-Interim reanalysis: configuration and performance of the data assimilation system, *Q. J. Roy. Meteo. Soc. 137*, 553–597, 2011.

Dong, B., Sutton, R., Woolings, T., and Hodges, K. Variability of the North Atlantic summer storm track: mechanisms and impacts on European climate. *Environ. Res. Lett. 8*, 034037, 2013.

Garaboa-Paz, D., Eiras-Barca, J., Huhn, F., and Pérez-Muñuzuri, V. Lagrangian coherent structures along atmospheric rivers. *Chaos 25*, 063105, 2015.

García-Morales, M. and Dubus, L. Forecasting precipitation for hydroelectric power management: how to exploit GCM's seasonal ensemble forecasts, *International Journal of Climatology 27*, 1691–1705, 2007.

Haller, G., and Beron-Vera F.J. Geodesic theory of transport barriers in two-dimensional flows. *Physica D 241*, 1680–1702, 2012.

Hatzaki, M. and Renguang, W. The south-eastern Europe winter precipitation variability in relation to the North Atlantic SST. *Atmospheric Research 152*, 61–68, 2015.

Herrera, S., Gutiérrez, J.M., Ancell, R., Pons, M.R., Fías, M.D., and Fernández, J. Development and analysis of a 50-year high-resolution daily gridded precipitation dataset over Spain (Spain02), *Int. J. Climatol. 32*, 74–85, 2012.

Howden, S.M. Soussana, J.F., Tubiello, F.N., Chhetri, N., Dunlop, M., and Meinke, H. Adapting agriculture to climate change, *Proceedings of the National Academy of Science 104*, 19691–19696, 2007.

Huhn, F. von Kameke, A., Pérez-Muñuzuri, V., Olascoaga, M.J., and Beron-Vera, F.J. The impact of advective transport by the South Indian Ocean Countercurrent on the Madagascar plankton bloom, *Geophys. Res. Lett. 39*, L06602, 2012.

Koh, T.Y., and Legras, B. Hyperbolic lines and the stratospheric polar vortex, *Chaos 12*, 382–394, 2002.

Lehmann, J. and Coumou, D. The influence of mid-latitude storm tracks on hot, cold, dry and wet extremes. *Sci. Rep. 5*, 17491, 2015.

Lorenzo, M.N., Iglesias, I., Taboada, J.J., and Gómez-Gesteira, M. Relationship between monthly rainfall in northwest Iberian Peninsula and North Atlantic sea surface temperature. *International Journal of Climatology 30*, 980–990, 2010.

Meza, F.J., Hansen, J.W., and Osgood, D. Economic Value of Seasonal Climate Forecasts for Agriculture: Review of Ex-Ante Assessments and Recommendations for Future Research, *Journal of Applied Meteorology and Climatology 47*, 1269–1286, 2008.

Peacock, T. and Dabiri, J.O. Introduction to Focus Issue: Lagrangian Coherent Structures, *Chaos 20*, 017501, 2010.

Pierrehumbert, R.T., and H. Yang. Global chaotic mixing on isentropic surfaces, *J. Atmos. Sci. 50*(15), 2462–2480, 1993.

Rodríguez-Fonseca, B. and deCastro, M. On the connection between winter anomalous precipitation in the Iberian Peninsula and North West Africa and the summer subtropical Atlantic sea surface temperature *Geophysical Research Letters 29*, 1863, 2002.

Rodríguez-Fonseca, B., Suárez-Moreno, R., Ayarzagüena, B., López-Parages, J., Gómara, I., Villamayor, J., Mohino, E., Losada, T., and Castaño-Tierno, A. A Review of ENSO Influence on the North Atlantic. A Non-Stationary Signal. *Atmosphere 7*, 87, 2016.

Rutherford, B., G. Dangelmayr, and M.T. Montgomery, Lagrangian coherent structures in tropical cyclone intensification, *Atmos. Chem. Phys. 12*(12), 5483–5507, 2012.

Sadlo, F., and Peikert, R. Efficient visualization of Lagrangian coherent structures by filtered AMR ridge extraction, *IEEE Transactions on Visualization and Computer Graphics 13*, 1456–1463, 2007.

Saenz, J., Rodríguez-Puebla, C., Fernández, J., and Zubillaga, J. Interpretation of interannual winter temperature variations over southwestern Europe. *J. Geophys. Res. 106*, 20641–20651, 2001.

Seierstad, I.A., Stephenson, D.B., and Kvamsto, N.G. How useful are teleconnection patterns for explaining variability in extratropical storminess? *Tellus Ser. A 59*, 170–181, 2007.

Serrano, A., García, J.A., Mateos, V.L., Cancillo, M.L., and Garrido, J. Monthly Modes of Variation of Precipitation over the Iberian Peninsula. *J. Climate 12*, 2894–2919, 1999.

Shadden, S.C., Lekien, F., and Marsden, J. Definition and properties of Lagrangian coherent structures from finite-time Lyapunov exponents in two-dimensional aperiodic flows, *Physica D 212*, 271–304, 2005.

Tang, W., M. Mathur, G. Haller, D.C. Hahn, and F.H. Ruggiero, Lagrangian Coherent Structures near a Subtropical Jet Stream, *J. Atmos. Sci. 67*(7), 2307–2319, 2010.

Thomson, M.C., García-Herrera, R., and Beniston, M. eds. Seasonal Forecasts, Climatic Change and Human Health. New York: Springer. 234 pp, 2008.

Vicente-Serrano, S.M., and López-Moreno, J.I. Nonstationary influence of the North Atlantic Oscillation on European precipitation, *J. Geophys. Res. 113*, D20120, 2008.

Visbeck, M., Chassignet, E., Curry, R., Delworth, T., Dickson, B., and Krahmann, G. The Ocean's Response to North Atlantic Oscillation Variability. In: The North Atlantic Oscillation: Climate Significance and Environmental Impact, Hurrell, J.W., Y. Kushnir, G. Ottersen and M. Visbeck (eds) American Geophysical Union: Washington, DC; 113–146, 2003.

von Hardenberg, J., and A.F. Lunkeit, Transient chaotic mixing during a baroclinic life cycle, *Chaos 10*(1), 1054–1500, 2000.

Woollings, T., Hannachi, A., and Hoskins, B. Variability of the North Atlantic eddy-driven jet stream. *Q. J. R. Meteorol. Soc. 136*, 856–868, 2010.

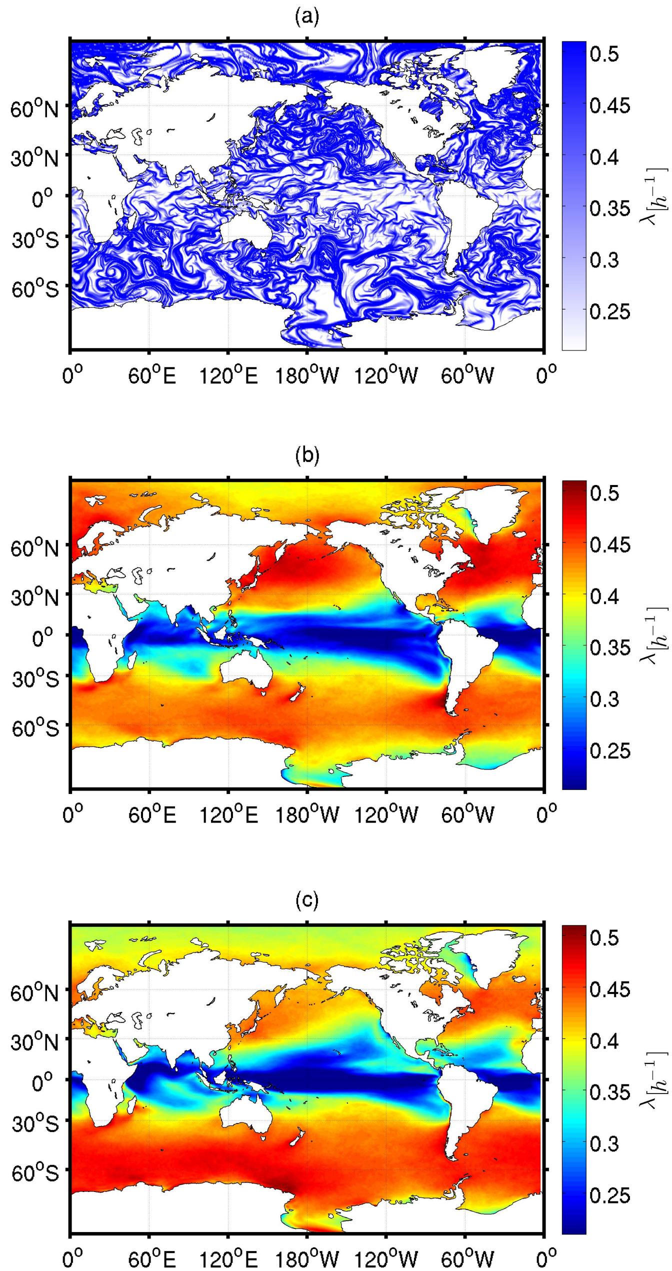

Figure 1. Finite-time Lyapunov exponents λ (a). Local maxima in the plot (darker colors) are potential repelling Lagrangian coherent structures. Mean FTLE climatology for periods January-March (b) and July-September (c) for the $1979 - 2008$ time series. $\tau = 5$ days.

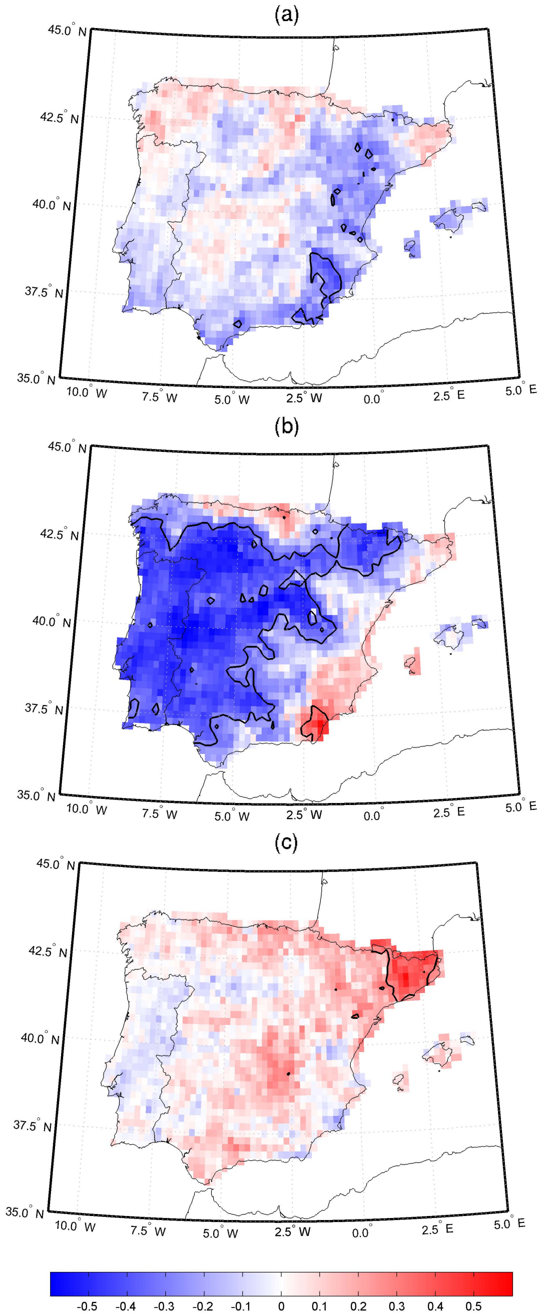

Figure 2. Correlation map between winter precipitation of the Iberian Peninsula and the FTLE anomalies for the Eastern Atlantic region ($[30°W, 0°W] \times [25°N, 65°N]$) for the three previous seasons; a) spring (AMJ), b) summer (JAS) and c) autumn (OND). The black lines mark the significant correlation at 95%.

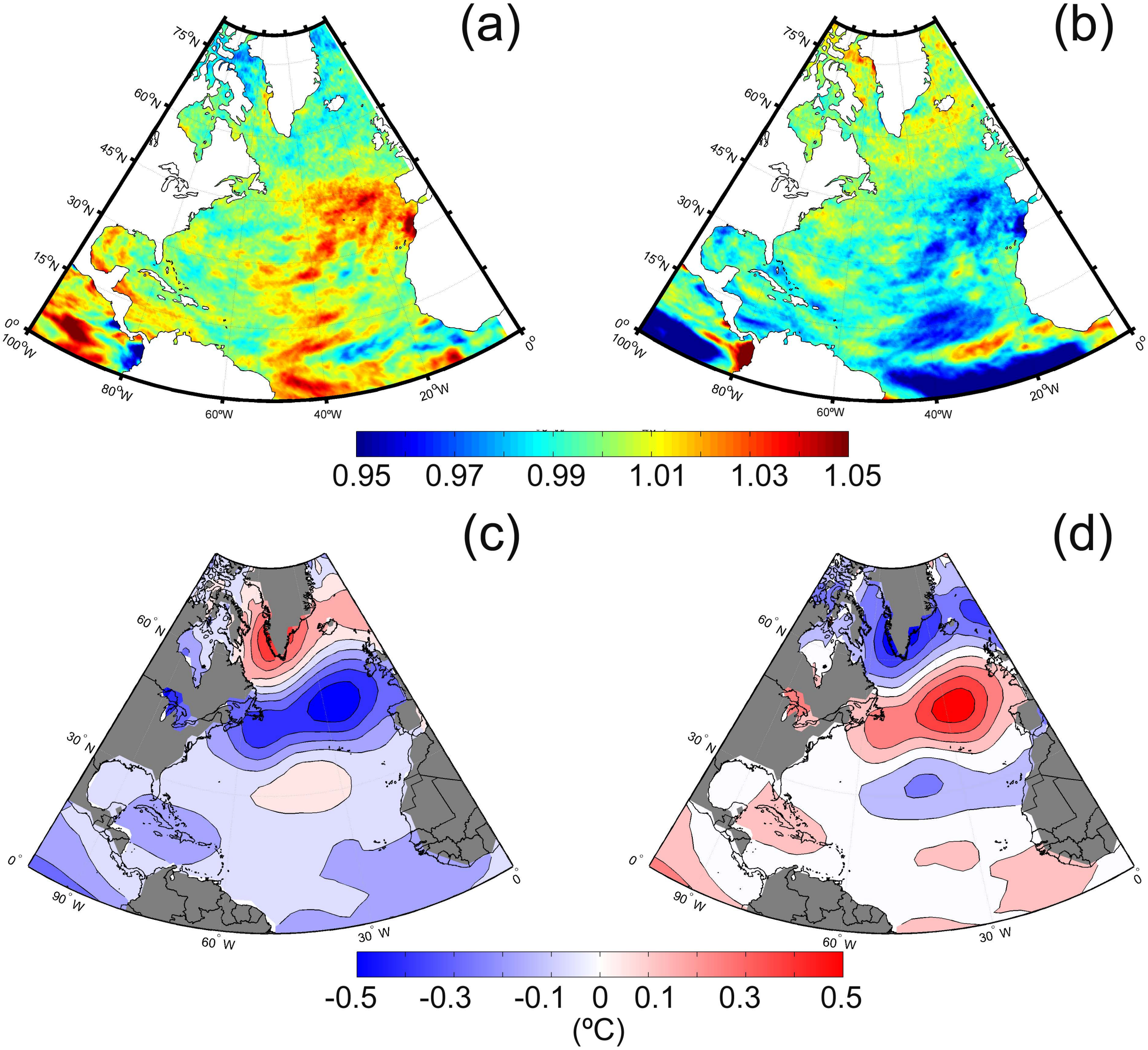

Figure 3. Ratio between the positive (a) and negative (b) summer FTLE anomalies and the global summer FTLE mean. Summer SST anomalies in the Atlantic ocean for years with positive (c) and negative (d) summer FTLE anomalies, respectively.

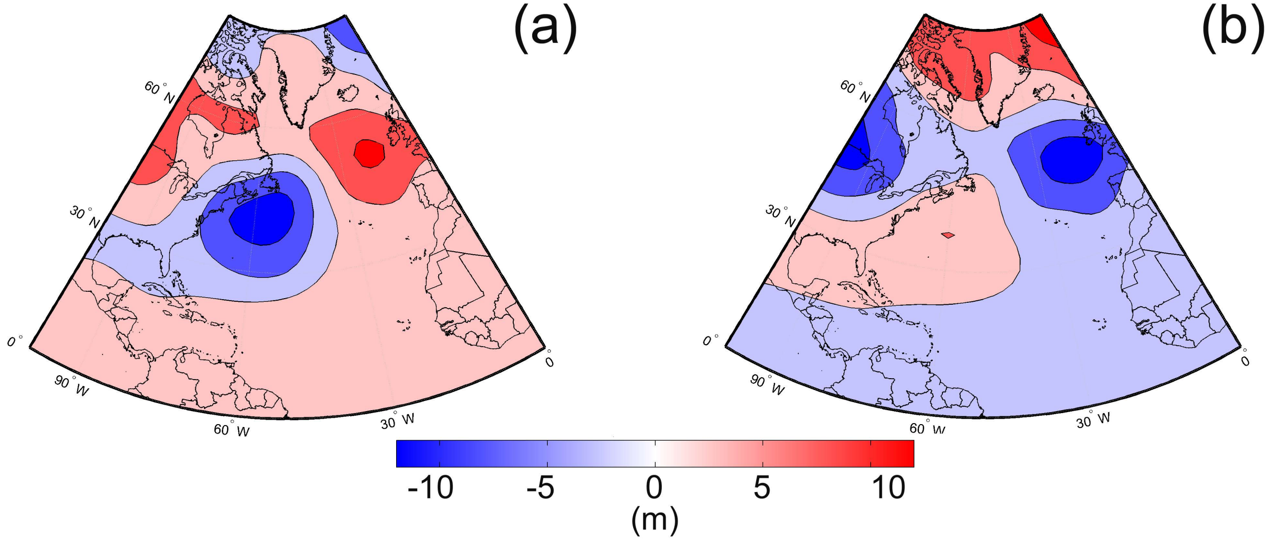

Figure 4. Geopotential at 500 hPa anomalies in the Atlantic for winter. (a) and (b) correspond to years with positive and negative summer FTLE anomalies, respectively.

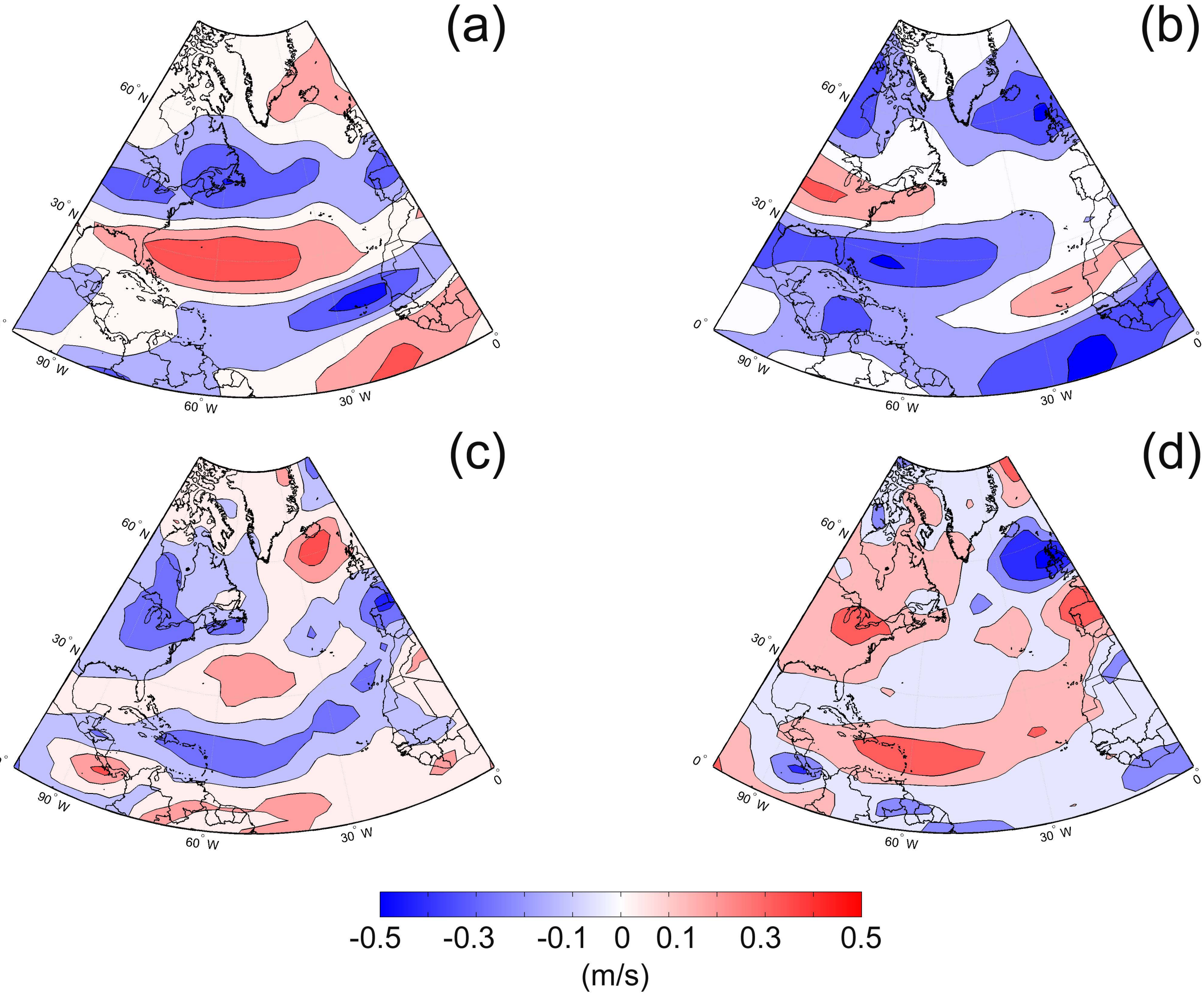

Figure 5. Wind speed anomalies in the Atlantic for winter. (a/b) and (c/d) correspond to years with positive/negative summer FTLE anomalies. Upper and lower maps correspond to 200 hPa and 850 hPa levels, respectively.